

Formation and evolution of compact binaries in globular clusters: I. Binaries with white dwarfs.

N. Ivanova^{1*}, C. O. Heinke^{2†}, F. A. Rasio², R. E. Taam², K. Belczynski^{3‡}, & J. Fregeau²

¹Canadian Institute for Theoretical Astrophysics, University of Toronto, 60 St. George, Toronto, ON M5S 3H8, Canada

²Northwestern University, Dept of Physics & Astronomy, 2145 Sheridan Rd, Evanston, IL 60208, USA

³New Mexico State University, Department of Astronomy, 1320 Frenger Mall, Las Cruces, New Mexico 88003-8001, USA

1 September 2018

ABSTRACT

In this paper, the first of a series, we study the stellar dynamical and evolutionary processes leading to the formation of compact binaries containing white dwarfs in dense globular clusters. We examine the processes leading to the creation of X-ray binaries such as cataclysmic variables and AM CVn systems. Using numerical simulations, we identify the dominant formation channels and we predict the expected numbers and characteristics of detectable systems, emphasizing how the cluster sources differ from the field population. We explore the dependence of formation rates on cluster properties and we explain in particular why the distribution of cataclysmic variables has only a weak dependence on cluster density. We also discuss the frequency of dwarf nova outbursts in globular clusters and their connection with moderately strong white dwarf magnetic fields. We examine the rate of Type Ia supernovae via both single and double degenerate channels in clusters and we argue that those rates may contribute to the total SN Ia rate in elliptical galaxies. Considering coalescing white dwarf binaries we discuss possible constraints on the common envelope evolution of their progenitors and we derive theoretical expectations for gravitational wave detection by LISA.

Key words: binaries: close – binaries: general – globular clusters: general – stellar dynamics.

1 INTRODUCTION

From the earliest observations of X-ray binaries in globular clusters (GCs) it has been noted that they must be very efficient sites for the production of compact binary systems (Clark 1975). The key to the overabundance of compact binaries in clusters, as compared to the field, is close stellar encounters. The processes that influence the binary population in dense stellar environments include the destruction of wide binaries (“ionization”), hardening of close binaries, physical collisions, and exchange interactions, through which low-mass companions tend to be replaced by more massive participants in the encounter. As a result of these processes, in the dense cores of globular clusters, binaries are strongly depleted and their period distribution is very different from that of a field population (Ivanova et al. 2005). This effect is stronger for binaries including a compact object, like cataclysmic variables (CVs).

The issue of the dynamical formation of CVs has been extensively discussed. Considering the CV formation via tidal captures, Bailyn et al. (1990) showed that dynamical formation of CVs is not expected because more massive donors lead to unstable mass transfer. On the other hand, Di Stefano & Rappaport (1994) predicted

the existence of many CVs formed via tidal captures, as many as an order of magnitude more than would be predicted by standard binary evolution, making CVs a probe of the dynamical processes in the cluster. Detection of CVs in globular clusters proved difficult (e.g. Shara et al. 1996), but a population was detected using the *Hubble Space Telescope* (Cool et al. 1995), along with a population of “nonflickerers” (Cool et al. 1998) which are understood to be young helium white dwarfs with C/O white dwarf companions (Hansen et al. 2003).

In the past few years, substantial progress has been made in optical identification of *Hubble Space Telescope* counterparts to *Chandra* X-ray sources in several GCs. Valuable information was obtained for populations of CVs, chromospherically active binaries and quiescent low-mass X-ray binaries (qLMXBs) (Grindlay et al. 2001; Pooley et al. 2002; Edmonds et al. 2003a; Bassa et al. 2004; Heinke et al. 2003). For the first time we can compare populations of such binaries in globular clusters (GCs) and in the Galactic field, and infer their rates of formation and population characteristics. In particular, 22 CVs have now been identified in 47 Tuc, allowing identification of several differences between typical CVs in globular clusters and CVs in the Galactic field. These differences include relatively high X-ray luminosities compared to field systems (Verbunt et al. 1997); a lack of novae, and of the steady, bright blue accretion discs signifying novalike CVs, in GCs

* E-mail: nata@cita.utoronto.ca

† Lindheimer Fellow

‡ Tombaugh Fellow

(Shara & Drissen 1995); relatively low frequencies of dwarf nova outbursts (DNOs), the typical identifiers of CVs in the Galactic disc (Shara et al. 1996); and a higher ratio of X-ray to optical flux than in most field CVs (Edmonds et al. 2003b). These differences produce puzzles: the lack of novae, novalikes, and DNO suggests very low mass transfer rates, while the high X-ray luminosities indicate moderate mass transfer rates. The X-ray to optical flux ratio suggests the CVs are DNe, but the lack of DNO argues against this. It was suggested that CV discs in GCs are more stable due to a combination of low mass transfer rates and moderately strong white dwarf magnetic moments (Dobrotka et al. 2005). This hints that the evolutionary paths of CVs in GCs and in the field are different. Comparisons of the numbers of CVs in clusters of different central densities also supports the idea that CVs are produced through dynamical interactions (Pooley et al. 2003), though there is an indication that CV production may depend more weakly on density than the production of low-mass X-ray binaries containing neutron stars (Heinke et al. 2003).

This is the first of two papers where we summarize results of our studies on compact binary formation in GCs, some preliminary results of which were reported in Ivanova et al. (2005); Ivanova & Rasio (2004, 2005). In this paper we focus on the formation of compact binaries with a white dwarf, and in the second paper (Paper II) we will describe dynamical formation and evolution of binaries with a NS companion. We explore a large spectrum of globular cluster models, where for the first time we take into account (i) the mechanism of binary formation through physical collisions using results from smoothed-particle hydrodynamics (SPH) and (ii) the effect of metallicity on the formation and subsequent evolution of close binaries. In Section 2 we provide a complete review of the physical processes of formation and destruction of mass-transferring WD binaries. In Section 3 we outline the methods and assumptions. The major formation channels, and population characteristics for CVs and AM CVn systems (double WD systems where one WD experiences Roche lobe overflow) in different clusters are presented and discussed in Section 4. We conclude in the last section by addressing the connection between our results and the observations.

2 MASS-TRANSFERRING WD-BINARIES IN A DENSE CLUSTER

There are several ways to destroy a primordial binary in a globular cluster. For instance, in a dense region a soft binary will very likely be “ionized” (destroyed) as a result of a dynamical encounter. A hard binary, in contrast, can be destroyed through a physical collision during the encounter. The probability of such an outcome increases strongly as the binary becomes harder (Fregeau et al. 2004). In addition to dynamical processes, a primordial binary can be destroyed through an evolutionary merger or following a SN explosion. Overall, even if a cluster initially had 100% of its stars in binaries initially, the binary fraction at an age of 10-14 Gyr will typically be as low as 10% (Ivanova et al. 2005).

To understand the evolution of a primordial binary in a dense environment and the probability of a binary becoming a CV, two steps are required: (i) compare the evolutionary time-scales with the time-scale of dynamical encounters; (ii) analyze what is the consequence of an encounter (this depends strongly on the hardness of the binary).

The time-scale for a binary to undergo a strong encounter with another single star (the collision time) can be estimated as $\tau_{\text{coll}} =$

$(n\Sigma v_\infty)^{-1}$. Here Σ is the cross section for an encounter between two objects, of masses m_i and m_j , with relative velocity at infinity v_∞ and is given as

$$\Sigma = \pi d_{\text{max}}^2 (1 + v_p^2/v_\infty^2), \quad (1)$$

where d_{max} is the maximum distance of closest approach that defines a significant encounter and $v_p^2 = 2G(m_i + m_j)/d_{\text{max}}$ is the velocity at pericenter. Assuming that a strong encounter occurs when the distance of closest approach is a few times the binary separation a , $d_{\text{max}} \leq ka$ with $k \simeq 2$, we obtain

$$\tau_{\text{coll}} = 3.4 \times 10^{13} \text{ yr } k^{-2} P_d^{-4/3} M_{\text{tot}}^{-2/3} n_5^{-1} v_{10}^{-1} \times \left(1 + 913 \frac{(M_{\text{tot}} + \langle M \rangle)}{k P_d^{2/3} M_{\text{tot}}^{1/3} v_{10}^2} \right)^{-1} \quad (2)$$

Here P_d is the binary period in days, M_{tot} is the total binary mass in M_\odot , $\langle M \rangle$ is the mass of an average single star in M_\odot , $v_{10} = v_\infty/(10 \text{ km/s})$ and $n_5 = n/(10^5 \text{ pc}^{-3})$, where n is the stellar number density.

The hardness of a binary system, η , is defined as

$$\eta = \frac{Gm_1m_2}{a\sigma^2\langle m \rangle}, \quad (3)$$

where a is the binary separation, σ is the central velocity dispersion, m_1 and m_2 are the masses of the binary components, and $\langle m \rangle$ is the average mass of a single star. Binaries that have $\eta < 1$ are termed soft, and those with $\eta > 1$ are termed hard.

2.1 Primordial CVs and AM CVns.

The typical formation scenario for CVs in the field (low density environment) usually involves common envelope (CE) evolution. In Fig. 1 we show parameters of primordial non-eccentric binaries that successfully become CVs. To obtain this parameter space, we used the binary population synthesis code `StarTrack` (Belczynski et al. 2002, 2005)¹. We evolved 5×10^5 binaries considering specifically that region of primordial binaries which, according to preliminary lower resolution runs, leads to CV formation. Our primary stars have masses between $0.5 M_\odot$ and $10 M_\odot$, the secondaries have masses according to a flat mass ratio distribution with initial periods distributed flatly between 1 and 10^4 days. For demonstration purposes in Fig. 1, we use initially circular orbits, because the parameters leading to different formation channels can be more clearly distinguished. For our actual cluster simulations we use eccentric binaries; in comparison to Fig. 1, eccentric primordial binaries can have higher initial periods and still produce CVs. Progenitors of CVs with a MS donor are located in the left bottom corner, with $M_p \lesssim 4 M_\odot$ and $\log P \lesssim 2.5$. In other cases the donor star is a red giant (RG) or a (sub)giant star in the Hertzsprung gap. For primordial binaries located in a small but dense area at the left middle part of Fig. 1, $\log P \sim 2.7$ and $M_p \sim 1 M_\odot$, a CE does not occur. We note that the lifetime of a binary in the CV stage with a RG donor is about 1000 times shorter than in the case of a MS donor.

In the core of a GC with core density $\rho_c \sim 10^5 \text{ pc}^{-3}$, a binary

¹ For the calculations in this study, we have used the `StarTrack` code prior to the latest release (Belczynski et al. 2005). However, the most important updates and revisions of input physics, in particular the ones important for evolution of binaries with white dwarfs, were already incorporated in the version we have used.

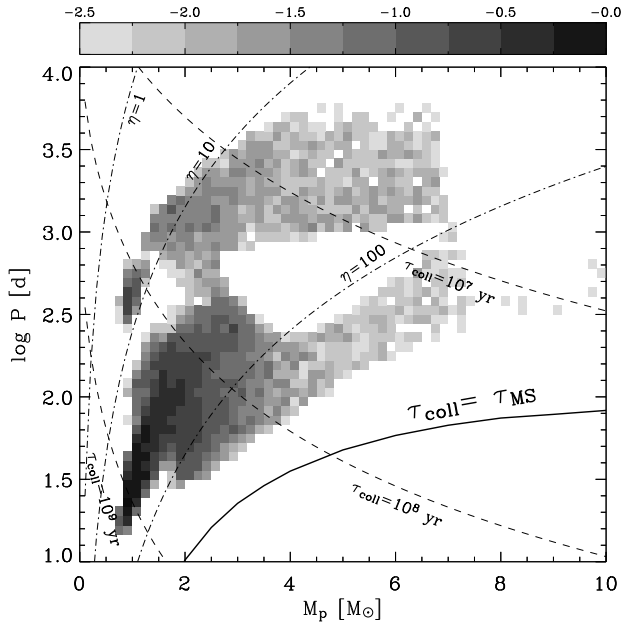


Figure 1. Distribution density of CV progenitors (initial masses of primary stars M_p and binary periods P) for non-eccentric binaries in the Galactic field, with $Z=0.001$. The total normalization of CV progenitors is scaled to unity, the grey color shows \log_{10} of the normalized distribution density. The thick solid line indicates the binary period where the collision time of the binary is equal to the main sequence lifetime of the primary (using a core number density $n = 10^5 \text{ pc}^{-3}$, a central velocity dispersion 10 km/s and an average object mass of $0.5 M_\odot$). Dash-dotted lines are lines of constant binary hardness and dashed lines are lines of constant collision time.

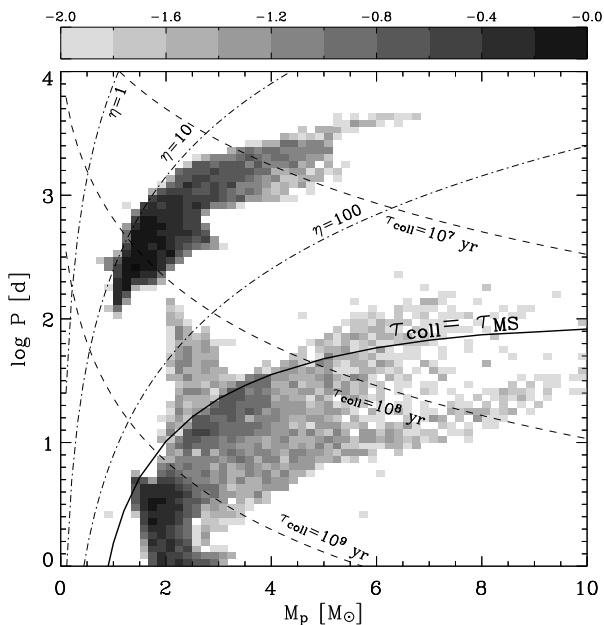


Figure 2. Distribution density of AM CVn progenitors (initial masses of primary stars M_p and binary periods P) for non-eccentric binaries in the Galactic field, $Z=0.001$. Notation as for Fig. 1.

with an initial period typical of a CV progenitor will experience a dynamical encounter before its primary leaves the MS (see Fig. 1, where all CV progenitors lie above the line indicating equality of τ_{coll} and τ_{MS}). The unaltered primordial channel for CV formation is therefore likely to succeed only for binaries that enter the dense cluster core after their CE event; the post-CE binary is compact enough to avoid an encounter. The contribution of the primordial channel depends therefore on the time – before or after the moment of CE – when primordial CV binaries will segregate into the central dense core. In more detail, an average initial binary in the GC is $\sim 0.7 M_\odot$, which is significantly smaller than the pre-CE mass of a primordial CV binary (see Fig. 1). Post-CE primordial CV binaries are also heavier than typical binaries in the halo (for which the average binary mass is $\sim 0.4 M_\odot$). In both cases, primordial CV binaries, as heavier objects, will tend to sink toward the cluster core on the cluster half-mass relaxation time.

The situation is similar for the formation of AM CVn systems from primordial binaries (see Fig. 2). In this case, the main formation channel requires the occurrence of two CE events (see also Belczynski et al. (2005a)), and the primordial binary is expected to be even wider. However, the second channel, with two stable MT stages (at the start of the RG stage of the primary, and when the secondary becomes a helium giant), is provided by relatively compact progenitor binaries. These binaries are expected to evolve in the same way in a GC as in the field.

2.2 Dynamical formation of CVs

A binary consisting of a MS star and a WD can be formed via several kinds of dynamical encounters: via an exchange interaction, via a tidal capture (TC) of a MS by a WD, or via physical collisions between a red giant (RG) and a MS star. A fraction of these dynamically formed MS-WD binary systems will start MT and become a CV. In this section we examine in detail the possible channels for CV creation.

The main angular momentum losses in a close MS-WD binary occur via magnetic braking (MB) and gravitational wave (GW) emission, both of which lead to orbital decay. In eccentric binaries, the binary orbital separation will be affected by tides, and the post-circularized periastron is larger than the pre-circularized periastron (unless tidal synchronization is significant). In Fig. 3 we show the maximum initial periods (at the moment of the binary formation) of a non-eccentric MS-WD binary that can start MT within 2 Gyr, and within 10 Gyr, due only to GW or only to MB (for illustrative purposes, we show time-scales for two prescriptions of magnetic braking, one is standard MB according to Rappaport et al. (1983) (RVJ) and the second is the MB based on dipole-field model according to Ivanova & Taam (2003) (IT03)). A maximum initial period such that a binary is able to start MT without having any other encounters is only ~ 2 days. On Fig. 4 we again show the maximum initial periods of binaries that may start MT, but now including all angular momentum losses (GW, MB and tides), and compare the cases of non-eccentric and eccentric binaries. On this figure we also show the difference in maximum initial period between metal-poor and metal-rich GCs. In metal-poor clusters only stars with $M \lesssim 0.85 M_\odot$ have developed outer convective zones, allowing MB and convective tides to operate (Ivanova 2006). This effect can potentially be dramatic; for instance, among non-eccentric binaries with a MS star of $1 M_\odot$, the range of post-exchange periods that leads to CV formation is a factor of 6 larger if the donor has $Z=0.02$, compared to $Z=0.001$. For eccentric binaries, this ratio is higher, as tidal circularization via radiative damping will reduce binary ec-

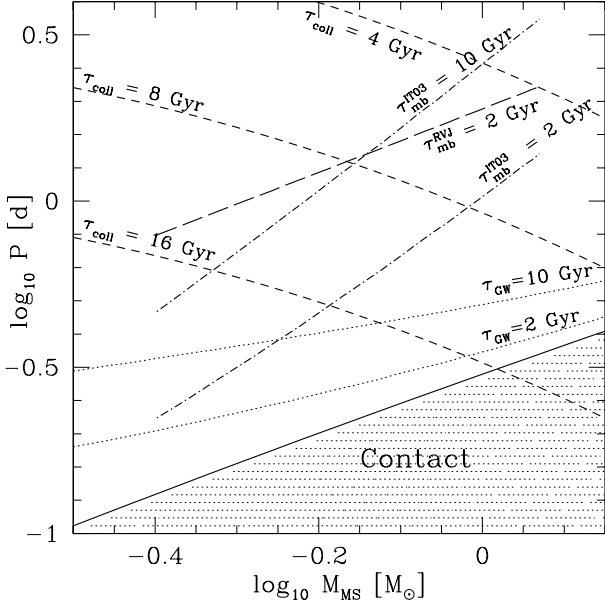


Figure 3. The fate of non-eccentric MS-WD binaries produced by, e.g., dynamical encounters, where the primary is a WD of $0.6 M_{\odot}$. P is the post-encounter (or post-CE) orbital period and M_{MS} is the mass of a MS secondary. The short-dashed lines show the binary periods for constant collision times and the dotted lines delineate the binaries that will shrink within 2 and 10 Gyr due to gravitational wave emission. The long-dashed line indicates the upper period limit for binaries that will begin MT within 2 Gyr with the RVJ MB prescription, while the dash-dotted lines indicate those that will begin MT within 2 and 10 Gyr with IT03 MB. Below the solid line the binary is in contact.

centricity (and therefore increase the periastron) more effectively than GW can shrink the binary orbit.

A circular binary is most likely to be formed via tidal capture (TC), where a post-capture circularization is assumed. Using the approach described in Portegies Zwart & Meinen (1993), we can estimate the post-capture binary parameters for a MS-WD binary (see Fig. 5, where WD mass is assumed to be $0.6 M_{\odot}$). The upper limit here corresponds to the closest approach at which tidal interactions are strong enough to make a bound system, and the lower limit corresponds to the closest approach at which the MS star overfills its Roche lobe by 1/3. We note that the parameter space for tidally captured binaries where the MS star does not overfill its Roche lobe at the closest approach is very small (see Fig. 3). We note that this is an optimistic estimate, as the captured star can also be destroyed during the chaotic phase of the tidal energy damping (Mardling 1995). Most tidally captured binaries can be brought to contact by MB before either the next encounter occurs, or the MS star evolves away from the MS.

An eccentric binary can be formed via an exchange encounter or a physical collision; eccentricity can also be increased via the cumulative effect of fly-by encounters. For binaries formed through MS-RG collisions, the post-exchange binary separation a_f as well as post-exchange eccentricity e_f depends on the closest approach p (Lombardi et al. 2006) and can be estimated using results of SPH simulations. These simulations were done for physical collisions of a NS and a RG, and therefore are not straightforwardly applicable for the physical collisions of a MS star and RG. We therefore study how strongly the choice of the treatment can affect the final results. We consider the two following prescriptions:

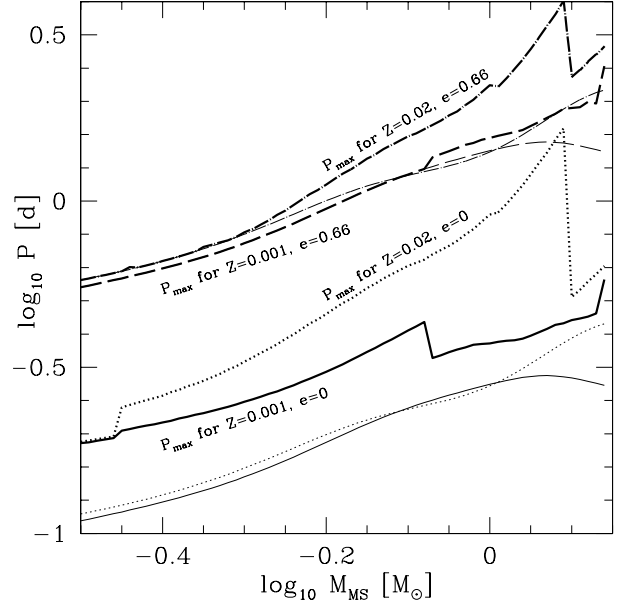


Figure 4. The fate of post-encounter MS-WD binaries where the primary is a WD of $0.6 M_{\odot}$, for post-exchange eccentricities 0 and 0.66. P is the post-encounter orbital period and M_{MS} is the mass of the MS secondary. Thick lines delineate the maximum periods for binaries which will begin MT within 2 Gyr. Thin lines of the same type show the period at which that binary will begin MT.

- Using a common-envelope (CE) prescription:

$$\frac{(M_{\text{rg}} + M_{\text{ms}})v_{\infty}^2}{2} + \alpha_{\text{CE}} \frac{GM_{\text{wd}}M_{\text{ms}}}{2a_f} = \frac{GM_{\text{rg}}(M_{\text{rg}} - M_{\text{wd}})}{\lambda R_{\text{rg}}} \quad (4)$$

Here M_{rg} , M_{ms} and M_{wd} are the masses of the RG, MS star, and RG core that will become a WD, in M_{\odot} ; R_{rg} is the RG radius; α_{CE} is the CE efficiency parameter; and λ is the CE parameter that connects a star's binding energy with its parameterized form. We assume that after a common envelope event the binary is not eccentric.

- Using parameterized results from SPH simulations:

$$e_f = 0.88 - \frac{p}{3R_{\text{RG}}} \quad (5)$$

$$a_f = \frac{p}{3.3(1 - e_f^2)} \quad (6)$$

As the parameterized SPH simulations were done for a limited set of mass ratios, we also check the energy balance. When we consider the case of the second treatment, we choose the minimum binary separation from eq. (4) and (6), as at small masses the extrapolated prescription from SPH simulations can lead to the formation of binaries with artificial energy creation. Also, in the case when a MS star at the pericenter overfills its Roche lobe, we destroy the MS star instead of forming a binary. This is consistent with the results of SPH simulations for physical collisions of a RG and a MS star (J. Lombardi 2005, priv. communication).

In Fig. 5 we also show possible binary periods for binaries formed via physical collisions with a red giant. Note that it is hard to form a relatively close MS-WD binary (one that is able to start MT within a few Gyr) with a WD more massive than $0.3 M_{\odot}$ via either prescription. Also, in binaries with the mass ratio $\gtrsim 3$, Roche lobe overflow leads to delayed dynamical instability and a binary

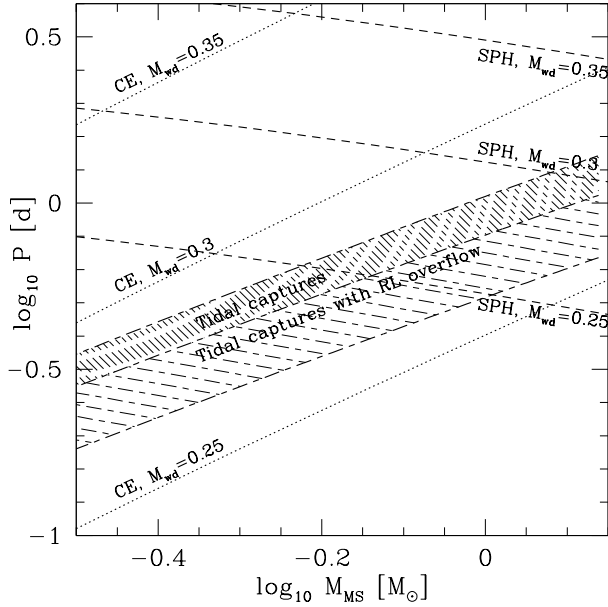


Figure 5. Formation of WD-MS binaries via physical collisions and tidal captures. The hatched area shows binaries formed via TC with a $0.6 M_{\odot}$ WD. In the dense hatched area, the MS star did not overflow its Roche lobe at the minimum approach during the TC. The dashed lines show binaries formed via physical collisions of a MS star and a $0.8 M_{\odot}$ RG, for different core masses, using parameterized results of SPH simulations (for illustrative purposes, we show only the case of the impact parameter to be 0.54 of the RG radius with corresponding post-collisional eccentricity of 0.7). The dotted lines show binaries formed via physical collisions of MS star and a $0.8 M_{\odot}$ RG, for different core masses, assuming common envelope approach ($\alpha_{CE} = \lambda = 1$).

merger. This limits the MS star mass to $\lesssim 0.9 M_{\odot}$. Therefore, the CV progenitors from the channel of physical collisions of RGs and MS stars are expected to initially have rather low mass WD accretors, and donor star masses $\lesssim 0.9 M_{\odot}$. Therefore, metallicity variations should not affect this channel strongly. The evolutionary stage during He core burning lasts almost the same time as the RG branch, however, He core stars of $\lesssim 2 M_{\odot}$ are a few times more compact than at the end of the RG branch and have a larger core than during RG evolution. Therefore a collision between a He core burning star and a MS star also favors the formation of a WD-MS binary that is close enough to become a CV. This channel mainly provides binaries with a WD mass at the start of accretion of about $0.5 M_{\odot}$ (just a bit above the core mass at the time of He core flash).

On the other hand, there are not many single WDs of such small masses present in a GC core. A WD with mass $\lesssim 0.3 M_{\odot}$ cannot (yet) be formed in single star evolution – it must evolve via a CE event or a physical collision. A binary containing such a WD is very hard and has $\tau_{\text{coll}} \geq 10$ Gyr. If an encounter occurs, it is more likely to result in a merger rather than an exchange. We therefore expect that most CVs with a low mass WD companion will be formed either through a CE event (in a primordial binary or in a dynamically formed binary with $P \sim 10 - 100$ days), or as a result of a physical collision, but not via direct exchange encounter.

A typical binary formed via an exchange encounter has $e \approx 0.7$. In order to become a CV within 2 Gyr (or before the next encounter), it should have a post-encounter period of a few days (see also Fig. 4). According to energy conservation during an exchange encounter (Heggie et al. 1996), and assuming that during

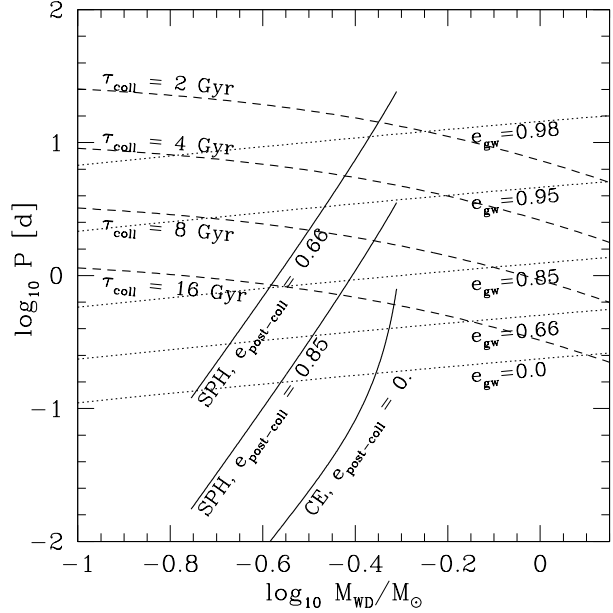


Figure 6. The fate of post-encounter WD-WD binaries where the primary is a WD of $0.6 M_{\odot}$. P is the post-encounter orbital period and M_{WD} is the mass of the WD secondary. The dashed lines show the binary periods for constant collision times and the dotted lines delineate the binaries that will begin MT within 2 Gyr due to GW emission for different post-encounter eccentricities that can be formed through a collision between a WD of $0.6 M_{\odot}$ and a RG of $0.8 M_{\odot}$ ($\alpha_{CE}\lambda = 1$).

an exchange encounter the less massive companion is replaced by the more massive intruding star, the post-encounter binary separation will be larger than pre-encounter. The domain of pre-encounter binaries that will be able to form a CV-progenitor binary via only exchange encounter is therefore limited to very short period binaries (with correspondingly long collision times), and these binaries are very likely to experience a physical collision rather than an exchange (Fregeau et al. 2004).

Let us consider the possibilities for an initially wider dynamically formed binary than shown on Fig. 4 to evolve toward MT. For definiteness, we consider a binary consisting of a $1 M_{\odot}$ MS star and a $0.6 M_{\odot}$ WD with an initial period of 10 days. There are two kinds of post-formation dynamical effects that can happen during fly-by encounters: (i) binary hardening; (ii) eccentricity pumping. Even if each hardening encounter could reduce the orbital separation by as much as 50%, the hardening of this binary from 10 days to 1 day (at this period MB starts to be efficient) will take about 20 Gyr. In the case of eccentricity pumping (assuming no binary energy change), the mean time between successive collisions stays at $\tau_{\text{coll}} \leq 1$ Gyr and therefore a binary can experience many encounters. If the acquired eccentricity $e \geq 0.95$, the binary can shrink through GW emission even if its initial period is larger than 10 days. The last possibility for such a wide dynamically formed binary to become a CV is a CE event that happens in a post-exchange MS-MS binary.

2.3 Dynamical formation of AM CVns

For the evolution of WD-WD binaries, we adopt that only GW are important as a mechanism of angular momentum loss and neglect

the possibility of tidal heating. The maximum possible periods for different post-encounter eccentricities are shown on Fig.6.

Let us first examine a WD-WD binary formation via direct exchange. Again, as in the case of MS-WD binaries, a typical eccentricity is $e \sim 0.7$ and the separation is comparable to the pre-exchange separation. The collision time for both pre-encounter and post-exchange binaries is so long that both binary hardening and exchanges are very rare events. The main difference with MS-WD binaries is that post-exchange WD-WD binary periods that will allow a binary to evolve to mass transfer (MT) are several times smaller for the same eccentricities. Therefore, the exchange channel producing a post-exchange binary consisting of two WDs seems to be very unlikely.

A more important channel seems to be the case of an exchange encounter that leads to the formation of a MS-WD binary. If the MS star is massive enough to become a RG during the cluster lifetime, such a binary can evolve through CE and form a close WD-WD binary.

The second important channel is again a physical collision, involving a single WD with a RG (see Fig. 6, where we show possible outcomes of a such a collision). We note that both treatments (parameterized SPH results and CE prescription) lead to the formation of WD-WD binaries that are roughly equally likely to start the MT.

We therefore expect that only a post-CE system can become an AM CVn, where the post-CE system could be from a primordial binary, a post-collision binary, or a dynamically formed binary.

3 METHODS AND ASSUMPTIONS

For our numerical simulations of globular clusters we use a Monte Carlo approach described in detail in Ivanova et al. (2005). The method couples the binary population synthesis code `StarTrack` (Belczynski et al. 2002, 2005), a simple model for the cluster, and a small N -body integrator for accurate treatment of all relevant dynamical interaction processes (`FewBody`, Fregeau et al. 2004). The main update of the code is the treatment of physical collisions with a RG, for which we now use the parameterized results of SPH simulations from Lombardi et al. (2006) as described in §2.2. In our code we keep a complete record of all events that happen to any cluster star, dynamical (like collisions, tidal captures and exchanges, as well as changes of the binary eccentricity or the binary separation after a fly-by encounter), or evolutionary (like common envelope events, mass transfers, or SN explosions). This helps to analyze the final populations and understand what factors played the most significant role in their formation.

The “standard” cluster model in our simulations has initially $N = 10^6$ stars and initial binary fraction of 100%. The distribution of initial binary periods is constant in the logarithm between contact and 10^7 d and the eccentricities are distributed thermally. We want to stress here that about 2/3 of these binaries are soft initially (the binary fraction provided by only hard binaries gives an initial binary fraction of about 20% if the 1-D velocity dispersion is 10 km/s) and most very tight binaries are destroyed through evolutionary mergers. Our initial binary fraction is therefore comparable to the initial binary fractions that are usually used in N -body codes, where it is assumed for simplicity that very soft binaries will not live long as binaries and will only slow down the simulations. For more detailed discussion on the choice of the primordial binary fraction, see Ivanova et al. (2005).

For single stars and primaries we adopted the broken power law initial mass function (IMF) of Kroupa (2002) and a flat mass-

ratio distribution for secondaries. The initial core mass is 5% of the cluster mass and, assuming initial mass segregation, an average object in the core is about twice as massive as an average cluster star. At the age of 11 Gyr the mass of such a cluster in our simulations is $\sim 2 \times 10^5 M_\odot$ and is comparable to the mass of typical globular clusters in our Galaxy.

We adopt a core number density $n_c = 10^5 \text{ pc}^{-3}$ (this corresponds to $\rho_c \approx 10^{4.7} M_\odot \text{ pc}^{-3}$ at the ages of 7-14 Gyr), a half-mass relaxation time $t_{\text{rh}} = 1$ Gyr and a metallicity $Z = 0.001$. The characteristic velocities are taken as for a King model $W_0 = 7$ for the cluster of this mass. We take a one-dimensional velocity dispersion $\sigma_1 = 10$ km/s and an escape velocity from the cluster $v_{\text{esc}} = 40$ km/s. If, after an interaction or SN explosion, an object in the core acquires a velocity higher than the recoil velocity $v_{\text{rec}} = 30$ km/s, an object is moved from the core to the halo. The ejection velocity for objects in the halo is $v_{\text{ej,h}} = 28$ km/s.

In addition to the “standard” model we also considered cluster models with the following modifications:

- a metal-rich cluster with $Z = 0.02$ (“metal-rich”);
- central density $n_c = 10^4 \text{ pc}^{-3}$ (“med-dens”) or $n_c = 10^3 \text{ pc}^{-3}$ (“low-dens”)
- initial binary fraction 50% (“BF05”);
- RVJ magnetic braking (“fast MB”);
- treatment of physical collision using a CE prescription (“CE coll”);
- 47 Tuc-type cluster, characterized by a higher density $\rho_c = 10^{5.2} M_\odot \text{ pc}^{-3}$, higher metallicity $Z = 0.0035$, $\sigma_1 = 11.5$ km/s, $v_{\text{esc}} = 57$ (with the recoil velocity of 52 km/s and $v_{\text{ej,h}} = 24$ km/s) and $t_{\text{rh}} = 3$ Gyr (“47 Tuc”).

“47 Tuc” model describes the GC where currently the largest CV population is identified. In order to find a better match with the observations, we examined several variations of this model. In particular, we considered a model with an initial binary population of 50% (“47 Tuc+BF05”), and a model with an initial binary population is 50%, and the initial core has a smaller mass - 2%, reflecting the effect of a longer half-mass relaxation time on the initial population (“47 Tuc+SCBF05”). We also examined the sensitivity of the final CV production to the CE efficiency parameter, considering the case with $\alpha_{\text{CE}}\lambda = 0.1$ (“47 Tuc+ $\alpha_{\text{CE}}\lambda$ ”).

In order to estimate the effects of dynamics on the population we also ran the same population as in our “standard” model ($Z=0.001$), but without dynamics (“non-dyn”). In order to compare to a field population, we considered the population of stars with solar metallicity $Z=0.02$ and with different times of star formation, assuming flat star formation rate through last 10 Gyrs (“field”). In “non-dyn” model all stars are formed at the zero age, like in GCs.

4 NUMERICAL RESULTS

4.1 Formation channels of CVs

4.1.1 Main formation channels in the “standard” model

In Fig. 7 we show the formation channels for all CVs that are present in a typical cluster (our “standard” model) at the age of 10 Gyr. Most of these CVs are too dim to be detected, and we consider separately the population of CVs that can be detectable according to present observational limits, considered specifically for the globular cluster 47 Tuc. For the limiting X-ray luminosity, we take $L_x \gtrsim 3 \cdot 10^{30} \text{ ergs s}^{-1}$ (Grindlay et al. 2001), and the limiting

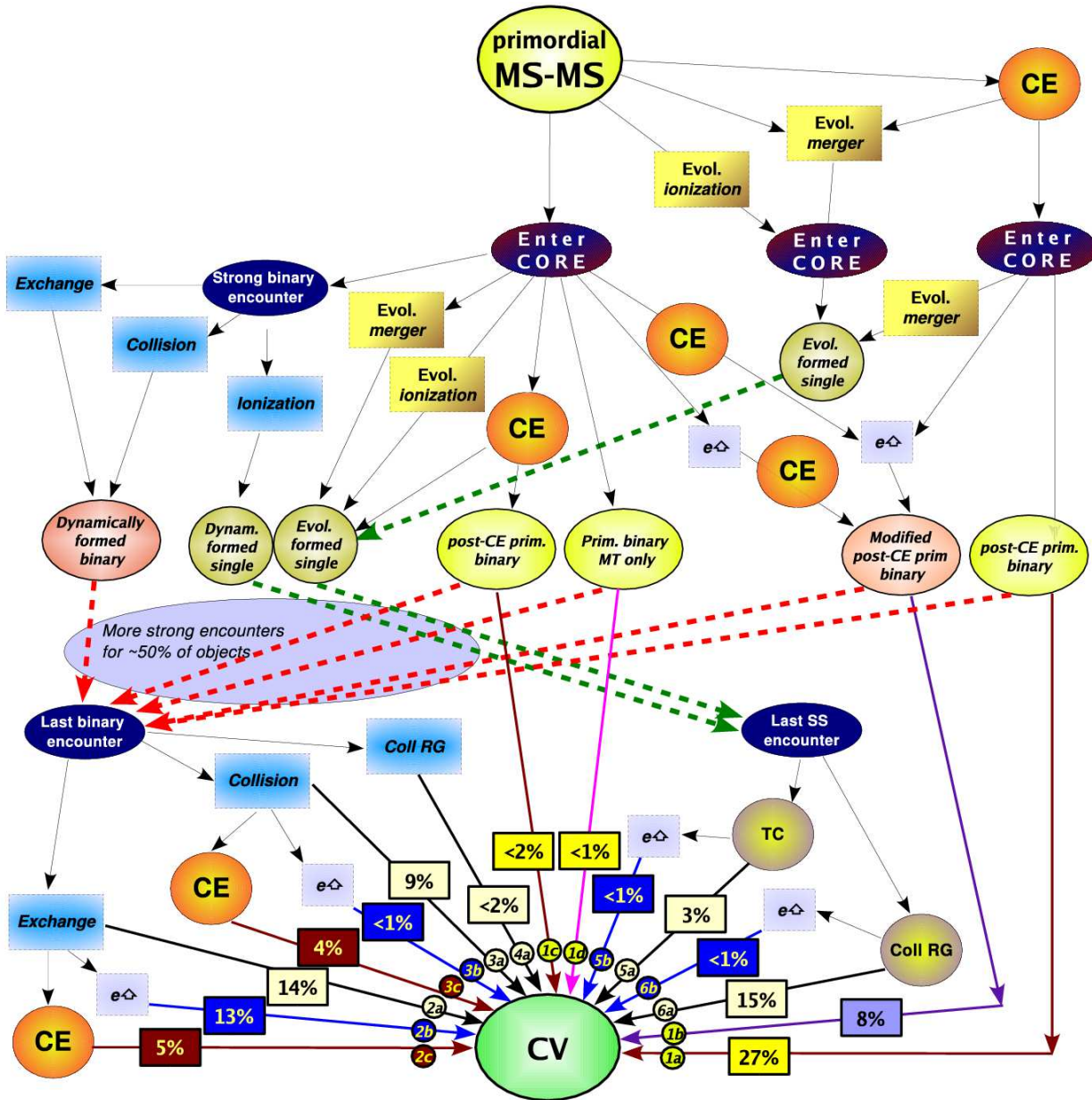


Figure 7. Main formation channels of all CVs that are present in a “standard” cluster at the age of 10 Gyr. Notations: numbers in squares represent contributions from different channels, small circles contain the labels for each channel. “CE” - common envelope, “Evol. merger” - evolutionary merger, “Evol. ionization” - destruction of the binary via SN explosion, “e \uparrow ” - increase of the eccentricity during fly-by encounters, “Strong binary encounter” - three- or four-body encounter with an outcome as exchange, binary destruction (“ionization”) or physical collision (“Collision”); “TC” - tidal capture, “Coll RG” - physical collision with a RG.

bolometric luminosity of the donor $L_d \gtrsim 0.06L_{\odot}$, set by the limiting magnitude of HST in the cluster core (Edmonds et al. 2003a).

We label channels in the following way: the first character indicates the last major dynamical event affecting the binary before it becomes a CV in the core, as follows: (1) entering the core (primordial binary); (2) companion exchange during a binary encounter; (3) merger during a binary encounter; (4) physical collision with a RG during a binary encounter that resulted in a tight binary formation with a RG core as a companion; (5) tidal capture; (6) physical collision of a single MS star with a single RG. The second character indicates a sub-channel by which the binary was modified after the last major dynamical event occurred: (a) stands

for all sub-channels where no strong evolutionary or dynamical event occurred; (b) eccentricity of the formed binary was increased via binary-binary encounters; (c) common envelope occurred; (d) a previous MT episode played the most important role in the orbital decay.

The *primordial channel (channel 1)* – provides 37% of all CVs that are present in the cluster core (42% of detectable CVs). We call this channel primordial as the binary keeps both its initial companions, and no mergers ever occurred to either of them. Only 3/4 of CVs formed via this channel are “purely” primordial in the sense that they did not experience a significant dynamical encounter throughout their life (1a, see also Fig. 7); most of these

“purely” primordial CVs evolved via CE before they entered the core. As was predicted in § 2.1, very few CVs come from the channel where CE occurred after a binary entered the core (**1c**). 1/5 of all primordial CVs would not evolve via CE or start a MT unless their eccentricity was increased via fly-by encounters (**1b**). A small fraction of primordial CVs evolved without a CE but with only a MT episode on to a MS star (**1d**), as was described in § 2.1.

The binary encounters (**channel 2, 3 and 4**) are responsible for the formation of 46% of all CVs, and the same fraction of detectable CVs. In most cases the binary that participated in the binary encounter was not a primordial binary, but a dynamically formed binary. In more than half of cases, a future accretor had been a companion in at least 3 different binaries before it acquired its final donor.

The most effective path is the *binary exchange channel (channel 2)* – it provides 32% of all CVs. Within this channel, $\sim 40\%$ of post-exchange binaries evolved toward the MT without further significant dynamical or evolutionary events (**2a**), in 20% of them CE occurred (**2c**) and in 40% of them the MT started as a result of the eccentricity pumping during subsequent fly-by encounters (**2b**). This is the most efficient channel for eccentricity pumping.

Exchange encounters that lead to CV formation typically occur between the following participants: (i) a single, relatively heavy WD (about $0.7 - 1.4 M_{\odot}$) and a MS-MS binary of total mass $\lesssim 1 M_{\odot}$; (ii) a single, relatively massive MS star (about turn-off mass) and a MS-WD or WD-WD binary. In the latter case, CE often follows the exchange encounter. The number of successful encounters between MS star and WD-WD binary is relatively small, and no successful four-body encounter occurred. Nearly all binaries that proceed via sub-channels 2a or 2b are WD-MS binaries, and all binaries in sub-channel 2c are MS-MS binaries after the last strong binary encounter. A post-exchange binary typically has a heavier WD than a primordial (post-CE) binary has.

A further 13% of CVs are formed in binaries that experienced a physical collision during the last three- or four-body encounter – *binary collisional channel (channel 3)*, while in 1% of cases a physical collision with a RG occurred during the encounter and a binary with the stripped RG core was formed (**channel 4**). In the evolution of post-collisional binaries the eccentricity change plays a smaller role compared to post-exchange binaries; MT is started due to the evolutionary angular momentum losses.

The *tidal capture channel (channel 5)* contributed very little in our standard model. When we looked at all CVs that were formed via TC over all GC ages, we find that a typical WD that captured a MS star is $\sim 1.0 \pm 0.2 M_{\odot}$. In our simulation we allowed a star to overflow its Roche lobe radius by up to 1/3 during the tidal capture encounter and survive. If all encounters where a MS star overfills its Roche lobe lead to the stars’ merger, then the contribution of tidal captures would be even smaller.

Finally, the *channel of physical collision with RGs (channel 6)* provides 15% of all CVs but much smaller fraction of detectable CVs. Eccentricity pumping played a very small role in both TC and physical collision channels. Typical participants of a successful physical collision (leading to CV formation) are a MS star of $0.3 - 0.9 M_{\odot}$ and a RG of about $1 - 1.7 M_{\odot}$ with a core around $0.3 M_{\odot}$ or a He core burning giant with a core mass around $0.5 M_{\odot}$. CVs formed by this channel are similar to post-CE CVs from primordial binaries. We also compared the results of CVs productions in our large model with 10^6 stars and in the model with three times less stars. We noted that, with the increase of the resolution, the total number and the number of detectable CVs per unit of the core mass

is slowly decreasing. Branching ratios between sub-channels within a channel can vary slightly, but an overall picture is the same.

We outline our main findings:

- Only $\sim 25\%$ of CVs were formed in binaries that would become CVs in the field.
- In $\sim 20\%$ of CVs the main reason for a binary to become a CV were fly-by encounters. These CVs cannot be predicted in simulations where only strong encounters are taken into account.
- In $\sim 15\%$ of CVs, the WD was formed during dynamical removal of the RG envelope. As this removal is not “clean”, and about $0.1 M_{\odot}$ (see Lombardi et al. 2006) can remain bound to the RG stripped core, the characteristics of the WD can differ from those formed via a common envelope.
- 60% of CVs did not evolve via CE, which is the most common formation channel for field CVs.
- Tidal captures did not play a significant role.

4.1.2 Formation channels in different clusters

In Table 1 we give details on the formation channels for different cluster models at the same age of 10 Gyr. We note that these numbers fluctuate with time and are not defined precisely (see more below in §4.1.3), however some trends can be identified. We also show the numbers of CVs that are formed in a metal-poor environment (“non-dyn”) and in the field. The definition of “detectable” CVs is not very consistent here, as observational limits for field CVs are not the same as for GCs (and much more poorly defined), but we use the same limits for comparison. It can be seen that dynamics in the “standard” model leads to an increase of the total CV production by less than a factor of two.

In the case of the “metal-rich” model, the turn-off mass at 10 Gyr is larger than in the “standard” model – there are more massive stars in the core; the ratio between the total numbers of CVs in two models is roughly the ratio between their turn-off masses at this age.

As was expected, the role of purely primordial CVs (channel 1a) decreases in importance when density increases (see “standard”, “med-dens” and “low-dens” models), although their absolute number is about the same for all three models – once a CV is formed outside the core, it is hard to destroy it in the core. On the other hand, the number of systems that experience CE after entering the core (1c) increases as the density decreases, since it is easier for pre-CE systems to survive in a less dense environment. The production of almost all channels via dynamical encounters decreases with density, except for channel 1b, where only non-strong encounters are involved. Overall, the total number of CVs in the core does not depend strongly on the core density, as the dynamical destruction of primordial binaries that would produce CVs, and the dynamical production of CVs, compensate each other.

The “fast MB” model shows the greatest difference with the “standard” model in the total number of CVs that are present in the cluster core: the “standard” model has about 3 times more CVs, both total and detectable, although the number of CVs that are ever formed in the core is slightly smaller. The “fast MB” model employs the prescription of MB with faster angular momentum loss than in the case of the standard model, and therefore the duration of the CV stage is shorter.

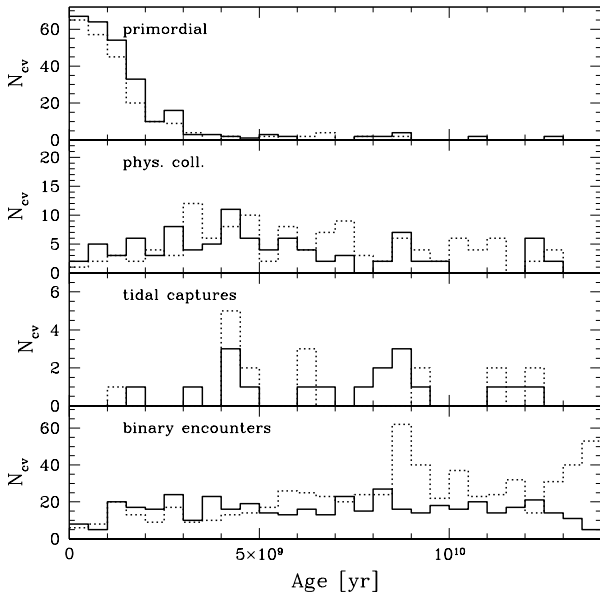
The “CE coll” model does not show significant differences with our “standard” model.

The “BF05” model shows that CV formation is reduced mainly for primordial CVs and for CVs produced via binary en-

Table 1. Formation channels of CVs that are present in the cluster cores of different models at the age of 10 Gyr.

channel	1a	1b	1c	2a	2b	2c	3a	3b	3c	4a	5a	6a	Total	Detec
standard	0.271	0.077	0.013	0.135	0.129	0.052	0.090	0.006	0.039	0.013	0.026	0.148	209	47
metal-rich	0.204	0.056	0.031	0.148	0.143	0.046	0.051	0.015	0.015	0.020	0.031	0.230	265	16
med-dens	0.327	0.253	0.167	0.111	0.012	0.056	0.031	0.019	0.006	0.006	0.000	0.006	193	35
low-dens	0.404	0.066	0.456	0.037	0.000	0.007	0.015	0.000	0.015	0.000	0.000	0.000	156	26
fast MB	0.190	0.103	0.017	0.086	0.190	0.172	0.034	0.017	0.000	0.017	0.052	0.103	79	15
CE coll	0.212	0.106	0.006	0.159	0.194	0.041	0.041	0.029	0.029	0.006	0.000	0.176	230	47
BF05	0.206	0.119	0.024	0.135	0.135	0.056	0.040	0.032	0.024	0.024	0.008	0.175	162	36
47 Tuc	0.135	0.094	0.000	0.250	0.146	0.073	0.042	0.042	0.021	0.031	0.000	0.156	275	37
47 Tuc+BF05	0.143	0.057	0.014	0.171	0.143	0.029	0.014	0.043	0.029	0.000	0.043	0.300	190	35
47 Tuc+SCBF05	0.071	0.114	0.000	0.100	0.114	0.057	0.014	0.014	0.014	0.014	0.029	0.443	237	27
47 Tuc+ $\alpha_{\text{CE}}\lambda$	0.170	0.057	0.011	0.182	0.125	0.045	0.034	0.011	0.011	0.023	0.023	0.307	253	40
non-dyn													124	16
field													117	3

Notations for channels – see text in § 4.1.1 and also Fig. 7. “Total” is the number of CVs and “Detec” is the number of detectable CVs, both numbers are scaled per 50 000 M_{\odot} stellar population mass in the core.

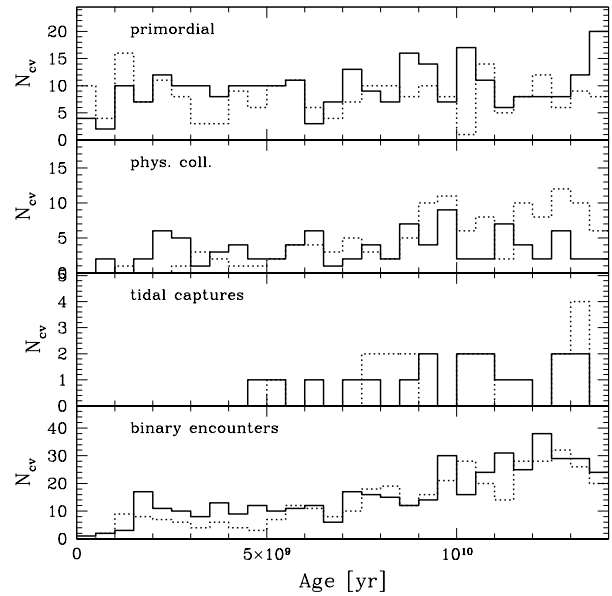

Figure 8. Formation of CVs via different channels. The solid line shows the case of “standard” model, dotted line shows “metal-rich”.

counters. The number of CVs produced via physical collisions between single stars is about the same.

The results for “47 Tuc” are due to a mixture of several conditions: the higher core number density favors dynamical formation, and the higher metallicity gives a wider mass range over which MB operates on the donor star. Variation of initial conditions, such as a smaller binary fraction, does not lead to significant differences except that the relative role of binaries becomes smaller than the role of physical collisions. Some decrease in the number of detectable CVs occurs when we start with a smaller initial core.

4.1.3 Formation channels at different cluster ages

In Fig. 8 we show the formation rate of CVs via different channels throughout the life of a cluster (indicating the time when a dynam-


Figure 9. Appearance of CVs (time that MT starts) formed via different channels. Notations as in Fig. 8

ical event occurred, or, for primordial binaries, the time when a CE happened). In Fig. 9 we show the rate of appearance of CVs (start of mass transfer) as a function of time.

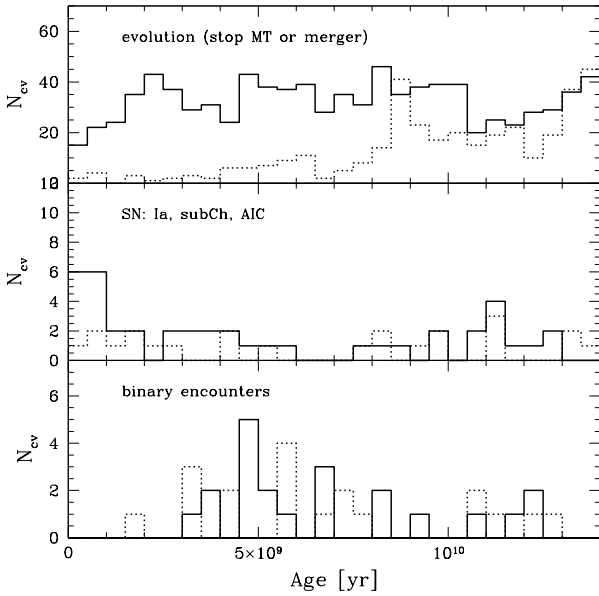
The primordial channel produces most of its CVs at the beginning of the cluster evolution, though the appearance of primordial CVs is distributed flatly in time. This contrasts with binary encounter channels, where the formation occurs rather flatly in time, but the rate of CV appearance grows after 7 Gyr. A similar delay in the appearance can be seen for CVs formed via tidal captures.

In Fig. 10 we show the number of CVs that stop MT for different reasons: (1) end of MT due to the star’s contraction (usually occurs with CVs where a donor is a RG) or evolutionary merger of the binary; (2) explosion of the WD as Ia SN or sub-Chandrasekhar SN explosion, or accretion induced collapse (AIC); (3) end of MT due to a strong dynamical encounter. Most CVs stop MT due to an

Table 2. Formation channels of CVs that are present in the “standard” cluster core at different ages.

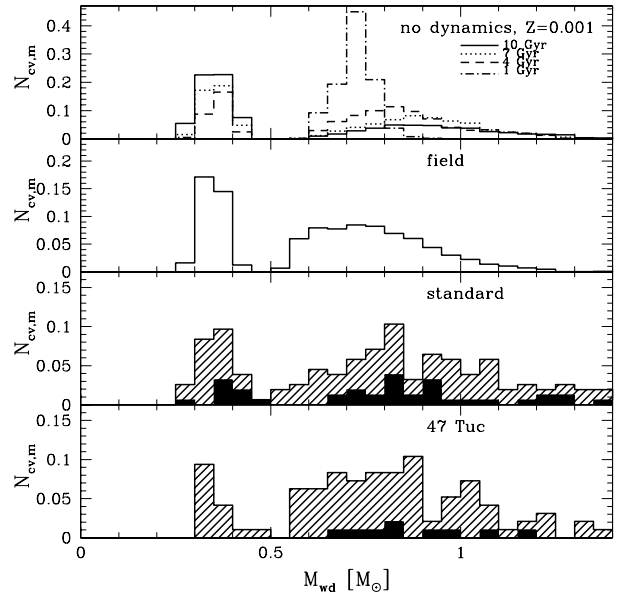
channel	1a	1b	1c	2a	2b	2c	3a	3b	3c	4a	5a	6a	Total	Det
1 Gyr	0.250	0.000	0.000	0.000	0.250	0.250	0.000	0.000	0.000	0.000	0.000	0.250	15	7
2 Gyr	0.111	0.074	0.037	0.259	0.111	0.185	0.000	0.000	0.037	0.000	0.000	0.185	84	37
3 Gyr	0.185	0.046	0.015	0.154	0.169	0.123	0.015	0.000	0.015	0.031	0.015	0.231	170	62
4 Gyr	0.200	0.078	0.022	0.167	0.133	0.133	0.022	0.000	0.011	0.022	0.011	0.200	203	76
5 Gyr	0.190	0.076	0.029	0.162	0.086	0.095	0.057	0.010	0.019	0.019	0.019	0.229	210	62
6 Gyr	0.214	0.077	0.026	0.162	0.103	0.060	0.051	0.009	0.026	0.026	0.017	0.231	211	56
7 Gyr	0.268	0.049	0.016	0.163	0.114	0.041	0.049	0.008	0.024	0.024	0.016	0.220	204	43
8 Gyr	0.284	0.061	0.014	0.128	0.122	0.068	0.054	0.007	0.041	0.020	0.014	0.182	228	44
9 Gyr	0.268	0.067	0.013	0.128	0.134	0.060	0.074	0.007	0.047	0.020	0.013	0.161	214	40
10 Gyr	0.271	0.077	0.013	0.135	0.129	0.052	0.090	0.006	0.039	0.013	0.026	0.148	209	47
11 Gyr	0.253	0.084	0.006	0.157	0.139	0.054	0.078	0.006	0.042	0.012	0.030	0.139	212	51
12 Gyr	0.209	0.088	0.005	0.165	0.181	0.049	0.066	0.016	0.033	0.005	0.027	0.154	221	41
13 Gyr	0.203	0.091	0.005	0.188	0.162	0.056	0.066	0.030	0.030	0.010	0.025	0.132	228	34
14 Gyr	0.199	0.131	0.000	0.184	0.155	0.039	0.068	0.044	0.029	0.010	0.019	0.121	229	43

Notations are as in Table 1.

**Figure 10.** Destruction of CVs. Notations as in Fig. 8.

evolutionary reason, while the number of SN explosions is also relatively high and is comparable to the number of CVs destroyed by dynamical encounters (for more detail on how SN Ia are calculated, see §4.4 and Belczynski et al. 2005).

In Table 2 we show a detailed representation of CV formation by different channels in the “standard” model at different cluster ages. We note a peak in the number of detectable CVs at the age of 4 Gyr, and that the total number of CVs increases steadily until the age of 8 Gyrs and then stays constant. The weight of different channels in the relative numbers of appearing CVs does not change dramatically during the cluster evolution.

**Figure 11.** The mass-distribution of hydrogen accreting WDs. The hatched area corresponds to dynamically formed binaries; the solid filled area to systems formed directly from primordial binaries. The top panel shows the case with no dynamics (different ages), the second panel from the top shows the compiled field case, the third panel shows the core of the cluster in the “standard” model and the bottom panel shows the cluster core in the model “47 Tuc”.

4.2 Population characteristics of CVs

4.2.1 Periods and masses

On Fig. 11 and 12 we show mass and period distributions for “standard” and “47 Tuc” cluster models, as well as for the population evolved without dynamics. A remnant of the primordial population of CVs in cluster cores follows the distribution of primordial CVs evolved without dynamics at the same age. However the distribution of dynamically formed CVs shows signs of younger (non-dynamical) CV populations, and also is more populated at the high mass end. For 47 Tuc we also show the periods of the identified

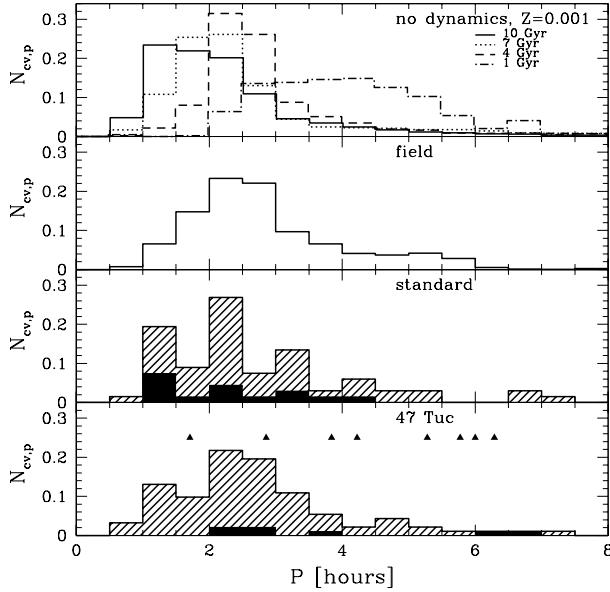


Figure 12. The period-distribution of hydrogen accreting WDs. The hatched area corresponds to dynamically formed binaries; the solid filled area to systems formed directly from primordial binaries. The top panel shows the case with no dynamics (different ages), the second panel from the top shows the compiled field case, the third panel shows the core of the cluster in the “standard” model and the bottom panel shows the cluster core in the model “47 Tuc”. Solid triangles indicates the periods of CVs that are identified in 47 Tuc from observations.

CVs, which have a distribution consistent with the period distribution of the “detectable” CVs in our simulations.

4.2.2 MT rates and X-ray luminosities

We compare the distribution of orbital periods versus 0.5–2.5 keV X-ray luminosity for our simulation of 47 Tuc and observations of CVs in globular clusters (see Fig. 13 and Fig. 14)². Observationally, few CVs have measured orbital periods. For real CVs with unknown periods, only the X-ray luminosity is shown. To obtain the X-ray luminosity of simulated CVs for comparison to observations, we use the accretion model from Patterson & Raymond (1985) for 0.5–4 keV and scale the luminosity to 0.5–2.5 keV assuming a flat energy distribution within the band:

$$L_x(0.5 - 2.5 \text{ keV}) = 0.066 \frac{GM_{\text{wd}} \dot{M}}{2R_{\text{wd}}}, \quad (7)$$

where \dot{M} is the mass transfer rate and R_{wd} is the radius of the WD. The simulations show reasonable agreement with the observations.

However, this picture so far does not explain the rare occurrence of DNOs in globular clusters CVs, in comparison to the field. Therefore, other properties of these systems must be explored to identify the distinguishing characteristics.

In Fig. 15 we show MT rates in CVs in “standard” model, in the “47 Tuc” model and for the field. Although MT rates in our GC simulations do not exceed $10^{-9} M_{\odot}/\text{yr}$, and field CVs can have

² Note that our “47 Tuc” represents a cluster similar to 47 Tuc but 5 times less massive

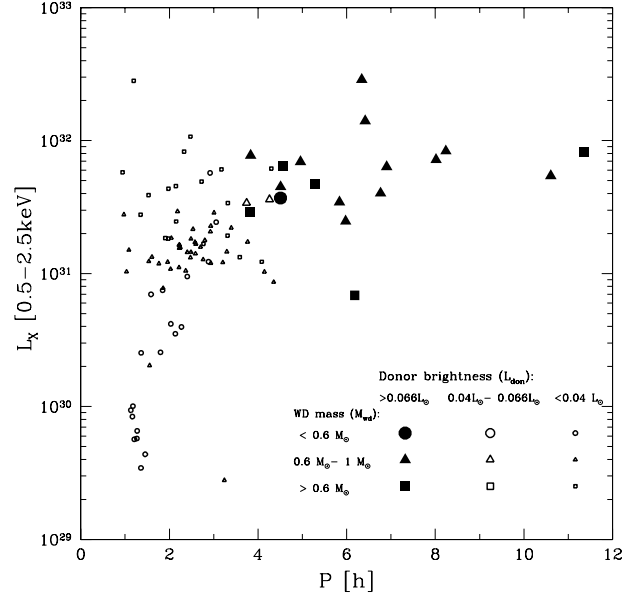


Figure 13. Simulated distribution of orbital periods versus 0.5–2.5 keV X-ray luminosity for “47 Tuc” model (at the age of 11 Gyr). Stars are CVs that could be detected, while open circles are CVs that cannot be detected (generally due to the optical faintness of the donor). The size of the symbol corresponds to the WD mass (the largest is for WDs more massive than $1 M_{\odot}$, the smallest symbol is for WDs less massive than $0.6 M_{\odot}$, and the medium symbol is for WDs with masses between 0.6 and $1 M_{\odot}$).

higher MT rates, this result may be due to small number statistics. We therefore do not find significant differences between MT rates in GC CVs and field CVs. For our GC CVs, all MT rates are such that the accretion disc is partially ionized and unstable, in accordance with the disc instability model. We adopt the viscosity parameters $\alpha_{\text{hot}} = 0.1$ and $\alpha_{\text{cold}} = 0.01$, for hot and stable disc states respectively. Therefore, all our CVs should produce DNOs.

Dobrotka et al. (2005) proposed that a combination of low MT rates and moderately strong magnetic fields can explain the absence of DNOs in GCs. Lower mass transfer rates would lead to a rarer occurrence of DNOs, and strong magnetic fields would lead to truncation of the inner disc keeping the disc in the cold stable state. As we do not find systematically lower MT rates for our GC CVs, (in fact our MT rates are two orders of magnitude higher than found in Dobrotka et al. (2005)), we estimated the minimum magnetic field required to suppress DNOs (see Fig. 16), using the criterion from (Dobrotka et al. (2005)):

$$B_{\text{supp}} \gtrsim 5.7 \times 10^5 \text{ G} \left(\frac{\dot{M}}{10^{-10} \frac{M_{\odot}}{\text{yr}}} \right)^{1.16} \left(\frac{M_{\text{wd}}}{M_{\odot}} \right)^{0.83} \left(\frac{0.01 R_{\odot}}{R_{\text{wd}}} \right)^3. \quad (8)$$

We find that B_{supp} is a slowly increasing function of the WD mass and, for most of the WDs with masses below $1 M_{\odot}$, is even below 10^6 G. WDs with $B \lesssim 10^6$ G are not regarded as highly magnetic. It can also be seen that a 10^7 G field is enough to prevent DNOs in all CVs with the WDs less massive than $1.1 M_{\odot}$ and the field of 10^8 G is strong enough to stop DNOs for WDs of all masses.

4.3 Formation Channels of AM CVns

In Table 3 we show the main formation channels for AM CVns that occur in different clusters, classifying channels in an analo-

Table 3. Formation channels of AM CVns that are present in the “standard” cluster core at 10 Gyr.

channel	1a	1b	1c	2a	2b	2c	3a	3b	3c	4a	5a	6a	Total
standard	0.385	0.068	0.000	0.051	0.090	0.030	0.013	0.013	0.064	0.064	0.009	0.265	316
metal-rich	0.379	0.089	0.000	0.031	0.071	0.022	0.018	0.004	0.009	0.009	0.000	0.348	303
med-dens	0.732	0.141	0.056	0.010	0.010	0.015	0.005	0.000	0.000	0.000	0.000	0.076	236
low-dens	0.680	0.085	0.178	0.008	0.004	0.036	0.000	0.000	0.000	0.000	0.000	0.178	283
fast MB	0.450	0.077	0.000	0.036	0.068	0.045	0.009	0.005	0.027	0.027	0.000	0.266	303
CE coll	0.474	0.123	0.000	0.035	0.082	0.023	0.006	0.012	0.018	0.018	0.012	0.211	231
BF05	0.271	0.090	0.005	0.053	0.080	0.016	0.011	0.032	0.011	0.011	0.000	0.404	242
47 Tuc	0.246	0.070	0.000	0.026	0.070	0.035	0.035	0.018	0.009	0.009	0.000	0.491	327
47 Tuc+BF05	0.174	0.110	0.000	0.018	0.101	0.037	0.000	0.009	0.009	0.009	0.009	0.514	296
47 Tuc+SCBF05	0.217	0.101	0.000	0.029	0.043	0.043	0.000	0.000	0.014	0.014	0.000	0.551	233
47 Tuc+ $\alpha_{\text{CE}}\lambda$	0.252	0.078	0.000	0.000	0.117	0.029	0.019	0.010	0.058	0.058	0.000	0.427	296
non-dyn													169
field													110

Notations for channels is the same as for CVs (see text in § 4.1.1 and also Fig. 7). “Total” is the number of AM CVns, the number is scaled per 50 000 M_{\odot} stellar population mass in the core.

gous manner to Sec. 4.1.1. The main differences with the formation of CVs are: (i) post-CE channels (including primordial) are more important; (ii) the role of physical collisions for AM CVns is increased; (iii) binary encounters played a much less significant role.

In most physical collisions the participants are a RG of 0.9 – 2.2 M_{\odot} (the core mass is 0.2 – 0.3 M_{\odot}) and a WD $\gtrsim 0.6 M_{\odot}$. In $\lesssim 20\%$ of physical collisions the participants are a He core burning giant of 1.7 – 2.2 M_{\odot} (the collision in this case leads to the formation of a He star of 0.4 – 0.55 M_{\odot}) and a heavier WD, generally $\gtrsim 0.9 - 1.1 M_{\odot}$.

Overall, this channel provides AM CVns with accretors of masses from 0.8 M_{\odot} to 1.4 M_{\odot} at a cluster age of 10 Gyr. The field population of AM CVns would have accretors with masses typically between 0.65 M_{\odot} and 1.0 M_{\odot} (Fig. 17, see also Nelemans et al. 2001; Belczynski et al. 2005b). The peak in the accretor mass distribution is shifted from $\sim 0.7 M_{\odot}$ in the field population to 0.9 M_{\odot} in the cluster population.

4.4 Explosive events

As the mass distribution of accreting WDs is shifted towards higher masses compared to the field population, it is important to check what effect this has on the rates of: (i) Type Ia supernova (SN Ia, here we mean the single degenerate channel only); (ii) double WD mergers (those for which the total mass $\geq M_{\text{Ch}} \simeq 1.4 M_{\odot}$); (iii) sub-Chandrasekhar supernovae; and (iv) accretion induced collapse (AIC).

The type of event that occurs depends on the mass and composition of the white dwarf and the rate of mass transfer. If this is a carbon-oxygen (CO) WD and experiences stable accretion, it will accumulate mass until it reaches the Chandrasekhar limit and then explodes as a type Ia supernova. In the case of specific MT rates the accretion leads to the accumulation of He in the shell (Kato & Hachisu 1999). If sufficient mass is accumulated, it will lead to the ignition of the CO or ONeMg core and disruption of the WD as a sub-Chandrasekhar-mass Type Ia supernova (see Taam 1980; Livne & Glasner 1991; Woosley & Weaver 1994; García-Senz et al. 1999; Ivanova & Taam 2004). In the case of accretion on to ONeMg WDs, upon reaching the Chandrasekhar limit the WD will undergo accretion-induced collapse and form a NS.

Table 4. Rate of explosive events.

event	SN Ia	supraCh	subCh	AIC	NS _{DD}	NS _{AIC}
standard	2.0	9.3	7.3	3.21	118	79.2
metal-rich	3.48	8.2	11.7	2.73	117	91.4
med-dens	0.48	2.4	8.0	1.45	89	64.7
low-dens	0.00	2.9	9.8	0.72	80	61.3
fast MB	3.48	8.2	11.7	2.73	117	91.4
CE coll	0.74	7.7	8.9	2.97	117	85.1
BF05	1.56	3.6	4.2	2.45	70	45.5
47 Tuc	1.22	4.9	9.3	2.44	88	70.3
47 Tuc+BF05	1.54	2.2	6.4	0.66	65	42.1
47 Tuc+SCBF05	0.66	2.4	6.2	0.88	50	36.3
47 Tuc+ $\alpha_{\text{CE}}\lambda$	2.20	3.2	8.8	1.71	87	59.6
non-dyn	0.00	0.7	3.2	0.00	70	69.4
field	0.50	7.7	15.1	1.58	122.17	22.8

“SN Ia” is the number of Type Ia SN (single-degenerate channel only), “supraCh” is the number of double WD mergers where the total mass is more than 1.4 M_{\odot} , “subCh” is the number of sub-Chandrasekhar nuclear runaways, “NS” is the number of NSs that can be potentially formed via double-degenerate (NS_{DD}) or AIC (NS_{AIC}) channels until the age of 10 Gyrs. For cluster models, rates and numbers are given per Gyr per 200,000 M_{\odot} total cluster mass and are averaged for the ages of 8-12 Gyr. For non-dynamical models, rates and numbers are given for the age of 10 Gyr and for the field model rates and numbers are given after 10 Gyr of continuous star formation.

If the donor is another WD and the mass transfer is not stable, the mass of the merger product can exceed the Chandrasekhar limit – these so-called supra-Chandrasekhar mergers could lead either to a Type Ia supernova (double-degenerate channel), or to a merger induced collapse of the remnant to form a NS and perhaps a millisecond radio pulsar (Chen & Leonard 1993). It was argued as well that in the latter case and, if one of the WD is magnetic, such mergers will lead to magnetar formation. Such objects may be responsible for the production of the giant flares emitted by soft γ -repeaters, which can be identified with early type galaxies. These flares may contribute to a fraction of the observed short duration burst population at higher redshift (Levan et al. 2006).

If NSs are born with natal kicks, most of them will be ejected

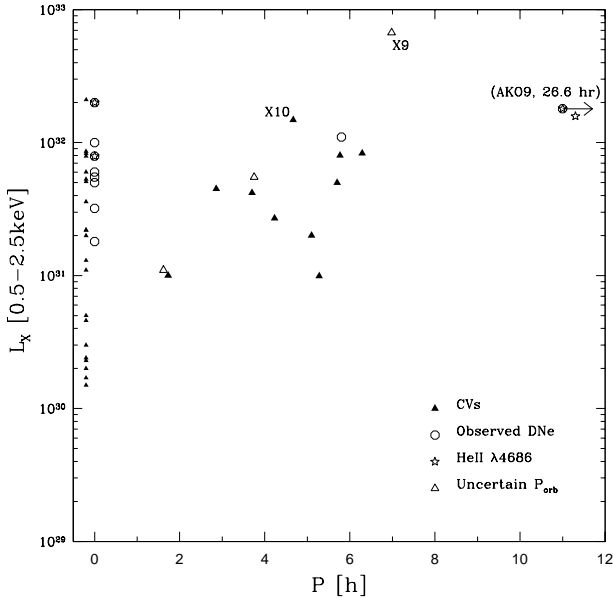


Figure 14. Observed distribution of orbital periods vs. 0.5-2.5 keV X-ray luminosity for CVs in globular clusters. Known CVs in globular clusters, with known X-ray luminosities but without known orbital periods, are plotted at $P=0$ hours or less. CVs that have undergone recorded dwarf nova outbursts are indicated with circles, CVs with strong He II $\lambda 4686$ emission (suggesting strong magnetic fields, see text) with stars (some are both). Three objects with uncertain periods or CV status (W34 in 47 Tuc might be a millisecond pulsar) are marked as open triangles; other CVs are indicated with filled triangles. Data include 23 CVs from 47 Tuc (Edmonds et al. 2003a,b), 8 from NGC 6397 (Edmonds et al. 1999; Grindlay et al. 2001; Kaluzny & Thompson 2003; Shara et al. 2005), 7 from NGC 6752 (Pooley et al. 2002; Bailyn et al. 1996), two from M22 (Pietrukowicz et al. 2005), two from M15 (Hannikainen et al. 2005), one from M5 (Hakala et al. 1997; Neill et al. 2002), one from M4 (Bassa et al. 2004), and one from M55 (Kaluzny et al. 2005).

from the shallow cluster potential, leaving few NSs to explain the observed number of millisecond pulsars (Pfahl et al. 2002). In the case of accretion or merger induced collapse, the NSs are likely to be formed without a significant kick (Podsiadlowski et al. 2004), and this can relieve the NS “retention problem”. If double WD mergers do not lead to collapse, they must contribute to the rate of Type Ia supernovae, with potential cosmological implications (for a review see Leibundgut 2001).

The production of supra-Chandrasekhar mergers in our galaxy was discussed in Hurley et al. (2002) and was estimated to be 2.6 per year in the Galactic disc (this is 8.6 per cluster per Gyr in our units). Several free parameters can have strong effects on this result, such as the common envelope prescription, the initial mass function, or the adopted star formation history. There are also differences between our models and those of Hurley et al. (2002): (i) their cut-off mass for WD binaries is at the initial mass of $0.8 M_{\odot}$; (ii) they choose $\alpha_{CE} = 3$; (iii) they adopted continuous star formation through 15 Gyr (c.f. ours 10 Gyr); and (iv) our model for accretion on to WDs is more up-to-date (for details, see Belczynski et al. 2005). Overall, we find that our formation rates for the field are not significantly different from those of Hurley et al. (2002) (see Table 4). We also find that our rates are smaller if the star formation is taken not as flat, but with one (or several) star formation bursts that ended several Gyrs ago.

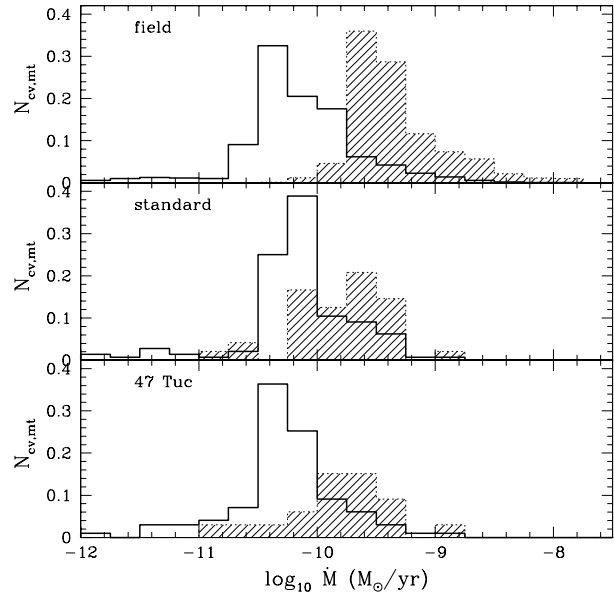


Figure 15. MT rates in CVs. Hatched areas indicate detectable CVs. For our no-dynamics model the detectable CV histogram is increased by a factor of 10, while for “47 Tuc” it is increased by a factor of 3. “47 Tuc” is shown at the age of 11 Gyr.

The enhanced production rate of double WD mergers in dense stellar clusters was first discussed in detail by Shara & Hurley (2002), who applied this to open clusters. They found that the supra-Chandrasekhar WD merger rate can be increased by an order of magnitude (although their statistics were based on only a few events). We did not find such an increase compared to the field population, where star formation is continuing, though we found some increase compared to the case without dynamical interactions (see Table 4). However, we note that our total number of supra-Chandrasekhar WD mergers is large. In fact, if indeed all those mergers lead to formation of NSs, and those NSs are retained by the cluster, then this channel provides about 6% of all NSs ever created. The NSs thus created become comparable in numbers to the NSs that were born with natal kicks and retained. The production of NSs via this channel can be reduced by reducing the efficiency of the common envelope. In this case, more binaries will merge during the CE phase and less supra-Chandrasekhar mergers will occur. We found however that even the reduction of $\alpha_{CE}\lambda$ to 0.1 led only to a moderate decrease of the “current” (at about 10 Gyr) production rate of supra-Chandrasekhar mergers, while their total production is only a bit smaller (see different models for 47 Tuc in the Table 4). In addition, the production of NSs via AIC is comparable to the production of NSs via merger induced collapse, and therefore also appears to be a significant source of NSs in GCs. The question of how many NSs can be created via different channels in GCs is very important, and will be addressed in more detail in Paper II.

We estimate the contribution of SN Ia produced in GCs to total galactic SN rates. Assuming that $\sim 3 \times 10^7 M_{\odot}$ is contained in galactic GCs (~ 150 galactic GCs), we find that the single-degenerate channel from GCs can provide at best 1 SN per $\sim 10^6$ yr per galaxy, and the contribution of GCs is only several times higher if the double-degenerate channel (supra-Chandrasekhar) also results in SN. In spiral galaxies the rate of SN Ia is 0.04-0.1 per cen-

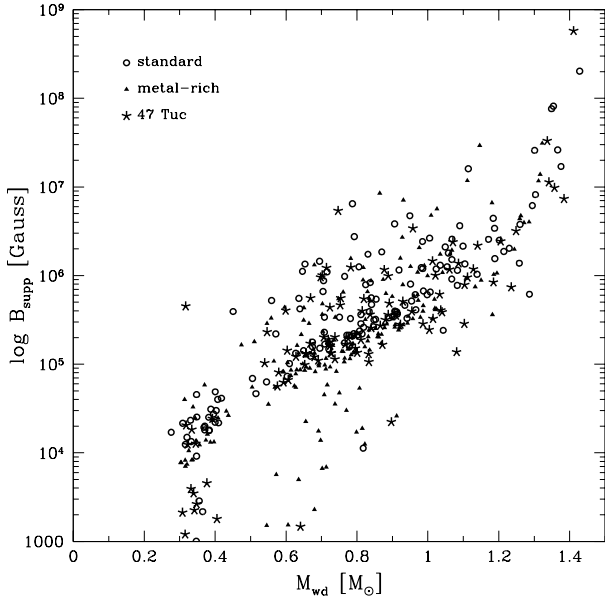


Figure 16. The minimum magnetic field B_{supp} required to prevent dwarf nova outbursts for CVs in our simulations. Open circles show CVs in the “standard” model, filled triangles show CVs in the “metal-rich” model, and stars indicate CVs in the “47 Tuc” model. “47 Tuc” is shown at the age of 11 Gyr, other models are shown at the age of 10 Gyr.

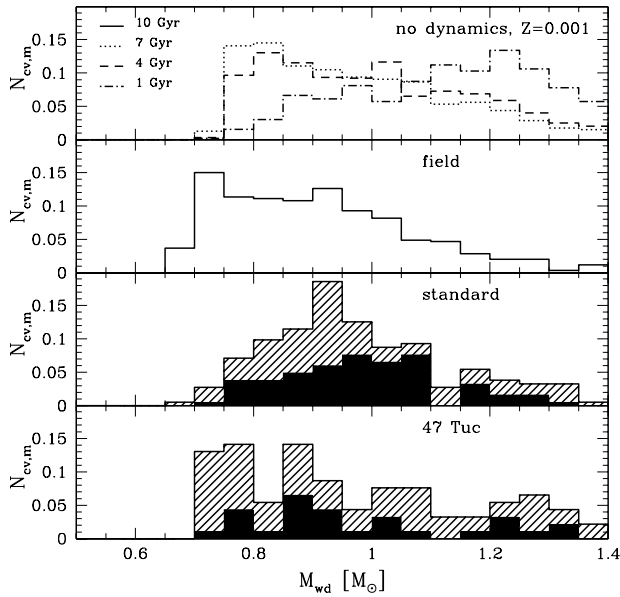


Figure 17. The mass-distribution of helium accreting WDs. The hatched area corresponds to dynamically formed binaries; the solid filled area to systems formed directly from primordial binaries. The top panel shows the case with no dynamics (different ages), the second panel from the top shows the compiled field case, the third panel shows the core of the cluster in the “standard” model and the bottom panel shows the cluster core in the model “47 Tuc”.

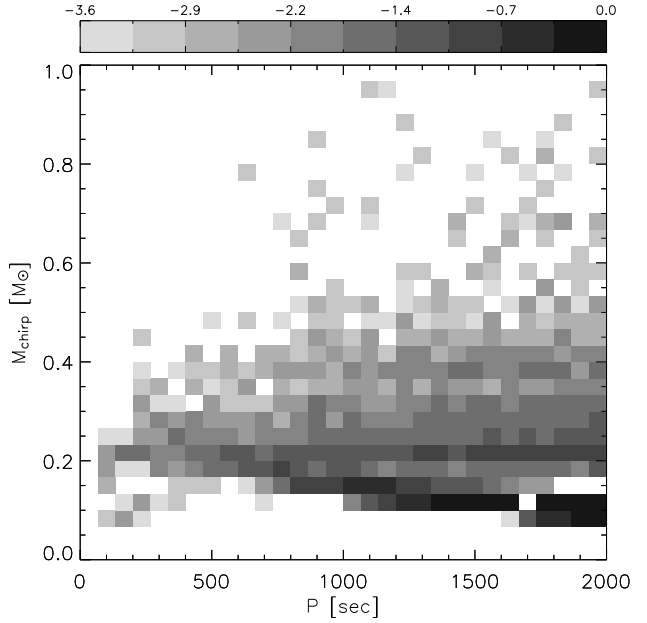


Figure 18. Distribution density (averaged over time) of LISA binaries, in the space of binary periods and chirp masses, from our “standard” model (integrated over cluster ages from 9 to 13 Gyr).

tury per galaxy (Mannucci et al. 2005), and therefore the contribution of GCs is not important. However, GCs can play a larger role in elliptical galaxies, where no star formation is going on and the rate of SN Ia provided by the field population is smaller. In addition, in ellipticals the specific frequency of GCs per galaxy luminosity unit is significantly higher than in spirals (up to 8.6 compared to 0.5 in Milky Way, see e.g. Kim & Fabbiano 2004). Also, it has been shown that the observational SN Ia rate consists of two components – a prompt piece that is proportional to the star formation rate, and an extended piece that is proportional to the total stellar mass (Scannapieco & Bildsten 2005). This is consistent with the behavior of the formation rates of both single degenerate and double degenerate channels in GCs, which peak during the first Gyr of the cluster evolution and have a flat distribution at later times. We therefore propose that GCs can increase the theoretically predicted rates of SN Ia in elliptical galaxies.

4.5 Coalescing compact binaries as LISA sources

AM CVns discussed in §4.3, as well as most double white dwarf mergers discussed in §4.4 (with the exclusion of a small fraction of mergers that are results of physical collision during hard binary encounters) are coalescing binaries driven by gravitational radiation. Prior to their mergers, or before and during the MT, they can be detectable as gravitational wave sources by LISA. Their detectability is significantly enhanced when their orbital periods become smaller than about 2000 s (Benacquista et al. 2001; Stroer et al. 2005), so their signals can be distinguished from the background noise produced by Galactic binaries. As the positional accuracy of LISA will be much greater for binaries with such short periods, these sources can be associated with specific globular clusters in our Galaxy.

From our simulations we find that at any given moment, a typical cluster of 200,000 M_{\odot} will contain 10 LISA sources on average, and at least 3 LISA binaries at any given moment; during 1 Gyr a cluster forms 180 LISA systems. A massive cluster like 47

Tuc, with mass $\sim 10^6 M_\odot$, will have at least 10 LISA sources at any given moment, and 40 LISA binaries on average. At an age of 10 Gyrs such a cluster can produce as many as 3-15 NS-WD LISA binaries per Gyr (a typical cluster produces 1-3 NS-WD coalescing binaries per Gyr).

With the total mass in GCs of about $3 \times 10^7 M_\odot$, as many as 1500 LISA binaries can be present in all Galactic GCs (this number will decrease if the CE efficiency is smaller). The most optimistic upper limit for the galactic formation rate of NS-WD binaries in GCs is several hundred per Gyr. The lifetime of a NS-WD binary in the LISA-band during the MT is $\sim 10^8$ yr. The time prior to the onset of MT depends on the binary eccentricity, but is usually much shorter (Ivanova et al. 2005). With our predicted formation rates, as many as 10-50 NS-WD LISA binaries can be detected in GCs. This number is probably too optimistic, as fewer than 10 ultra-compact X-ray binaries (mass-transferring NS-WD binaries with orbital periods less than an hour) have been identified in GCs, implying that the formation rate of LISA-sources should be smaller. (One explanation could be that many globular clusters are less dense than our “standard” model and NS-WD formation is thus less frequent.) We shall address the issue of the formation rates of binaries with NSs in more detail in Paper II. Here we will only note that the LISA binaries will spend most of their time in the LISA band among their MT tracks, with chirp masses $\lesssim 0.25 M_\odot$ (see Fig. 18).

5 DISCUSSION

With our simulations we predict that the formation rates of CVs and AM CVns in globular clusters are not very different from those in the field population. The numbers of CVs and AM CVns per mass unit are comparable to numbers in the field if the whole cluster population is considered, and they are only 2-3 times larger in the core than in the field. Dynamical formation is responsible only for 60%-70% of CVs in the core. This fraction decreases as the density decreases, and the role of primordial CVs becomes more important. We rule out tidal captures as an effective mechanism for CV formation in GCs unless the rate of TCs is significantly underestimated. Instead we propose that the population of GC CVs reflects a combination of primordial CVs, CVs in post-exchange binaries, and products of physical collisions of MS stars with RGs. There are also primordial CVs which are located in the halo and have never entered the core. The GC core density variation indeed does not play a very large role, in contrast to the case of NS binaries, where almost all systems are formed dynamically (Ivanova et al. 2005) and whose numbers have a strong dependence on the cluster collision rate (Pooley et al. 2003). We expect to have one detectable CV per 1000 M_\odot in the core of a typical cluster and about one detectable CV per 1000 – 2000 M_\odot in a 47 Tuc type cluster. Thus we predict 35-40 CVs in the core of 47 Tuc, in quite reasonable agreement with observations, where 22 CVs in 47 Tuc have been identified (Edmonds et al. 2003a). Even better agreement between our simulations and the observed number of CVs can be obtained if we assume that the initial core mass in 47 Tuc is smaller than 5% of the cluster.

Although the formation rates do not differ strongly, we found significant differences in the populations, and note that these differences may have observational consequences. Indeed, cataclysmic variables in globular clusters have an unusual array of characteristics, which make them difficult to classify as members of the standard classes of CVs recognized in the galaxy. Their X-ray luminosities seem to be rather high, compared with CVs in the

field (Verbunt et al. 1997). They exhibit dwarf nova outbursts only rarely, compared to well-studied dwarf novae: only 1 dwarf nova was found in 47 Tuc by Shara et al. (1996) in a survey which would have detected 1/3 of known dwarf novae if they were located in 47 Tuc, while Edmonds et al. (2003a) identify 22 firm CVs in 47 Tuc. Finally, the X-ray to optical flux ratios of CVs in globular clusters are relatively high, comparable to those of dwarf novae (Edmonds et al. 2003b).

One solution to this problem was the suggestion that CVs in globular clusters tend to be primarily magnetic in nature, compared to CVs in the field (Grindlay et al. 1995). Magnetic CVs have no discs (AM Her or polar CVs), or truncated discs (DQ Her CVs or intermediate polars, IPs), because of the effect of the WD magnetic field. As a result, the disc instability is nonexistent or suppressed. Magnetic CVs are believed to produce X-rays through an accretion shock above the polar cap, producing high X-ray luminosities, while nonmagnetic CVs produce an optically thick boundary layer, saturating their X-ray emission (Patterson & Raymond 1985). Strong He II λ 4686 lines were observed in the spectra of three CVs in NGC 6397 (Edmonds et al. 1999), indicating a strong source of FUV radiation. This FUV radiation could indicate either evidence for an intermediate polar interpretation, or a very high mass transfer rate; the second interpretation is favored for the FUV-bright, 27-hour period CV AKO9 in 47 Tuc (Knigge et al. 2003). Another argument in favor of the intermediate polar interpretation is the excess N_H (in addition to that expected along the line of sight) observed towards many CVs in 47 Tuc (Heinke et al. 2005). Excess N_H in CVs that are not observed at high inclinations has been considered a signature of the accretion curtains observed in the magnetic systems known as intermediate polars.

However, only two globular cluster CVs have shown clear evidence of magnetic fields in their X-ray lightcurves so far (X9 and X10 in 47 Tuc Grindlay et al. 2001; Heinke et al. 2005). This may not mean that these systems are not magnetic, since the number of X-ray photons detected from globular clusters is generally small (compared with nearby, well-studied CVs). In addition, it has been suggested that the accretion in SW Sex and VY Scl CVs is governed by the WD magnetic field, without evidence of pulsations (Rodríguez-Gil et al. 2001; Hameury & Lasota 2002). Another problem for the magnetic interpretation is that IPs tend to be optically brighter than typical CVs in globular clusters, which have lower ratios of X-ray to optical flux more typical of dwarf novae than IPs (Edmonds et al. 2003b). A final problem is the observation of dwarf nova outbursts in two of the three CVs in NGC 6397 possessing strong He II emission (Shara et al. 2005). A proposed resolution to these problems is a combination of a low mass transfer rate (which will reduce the optical brightness and increase the X-ray to optical flux ratio) with an intermediate polar nature (Edmonds et al. 2003b). Dobrotka et al. (2005) calculated the dwarf nova recurrence times for CV discs with various mass transfer rates and WD magnetic moments, and found a parameter space that fulfilled the requirements of globular cluster CVs. Left unanswered was why globular cluster CVs might tend to have stronger magnetic fields than field systems.

Our work provides a possible answer to this question. Globular cluster dynamics has a strong effect on the composition of the binaries that form CVs, tending to place more massive WDs into binaries that will become CVs (Fig. 11). Increasing the mass of WDs in CVs increases the energy that can be extracted at a given mass transfer rate, thus increasing the X-ray luminosity and X-ray to optical flux ratio of the CVs. This effect is complementary to the effects of higher magnetic fields.

However, higher mass WDs also have a higher probability of showing strong magnetic fields (Vennes 1999; Liebert et al. 2003; Wickramasinghe & Ferrario 2005). Thus the dynamical origin of WDs in globular cluster CVs may be responsible for the observational peculiarities of globular cluster CVs; their relatively high X-ray luminosities and X-ray to optical flux ratios, and their low rates of dwarf nova outbursts.

The tendency for higher mass white dwarf accretors in GC CVs in comparison to the field also affects the production of the superhump phenomenon. This behavior results from the precession of the outer disc due to the excitation of resonances within the disc caused by the 3:1 commensurability of motions in the disc with the companion's orbital period (see Whitehurst & King 1991). Such systems are characterized by mass ratios (of donor to accretor) of less than 0.25-0.33. Systems of this type in the field are rarely observed at orbital periods above the period gap, but the higher white dwarf masses of CVs in GCs would increase their likelihood in GCs.

We examined also several other consequences of having a dynamically modified population of close binaries including WDs. In particular, considering supra-Chandrasekhar mergers, we found that too many NSs may be formed if these mergers lead to merger-induced collapse. We suggest that either this mechanism does not lead to NS formation, or the CE efficiency is overestimated. By our estimates, GCs do not contribute strongly to the SN Ia rates in spiral galaxies, however they may significantly increase these rates in elliptical galaxies. We have also shown that GCs can be excellent sites for LISA observations since many GCs will contain several LISA sources at any given moment, although most of those systems will have low chirp masses.

ACKNOWLEDGMENTS

This work was supported by NASA Grant NAG5-12044 (FAR), NSF Grant AST-0200876 (RET), and Chandra Theory Grant TM6-7007X (JF) at Northwestern University, KB acknowledges support by KBN grant IP03D02228. All simulations were performed on the McKenzie cluster at CITA which was funded by the Canada Foundation for Innovation.

REFERENCES

- Bailyn C. D., Grindlay J. E., Garcia M. R., 1990, *ApJL*, 357, L35
 Bailyn C. D., Rubenstein E. P., Slavin S. D., Cohn H., Lugger P., Cool A. M., Grindlay J. E., 1996, *ApJL*, 473, L31+
 Bassa C., Pooley D., Homer L., et al. 2004, *ApJ*, 609, 755
 Belczynski K., Benacquista M., Larson S. L., Ruiters A. J., 2005a, *astro-ph/0510718*
 Belczynski K., Benacquista M., Larson S. L., Ruiters A. J., 2005b, *ArXiv Astrophysics e-prints*
 Belczynski K., Bulik T., Ruiters A. J., 2005, *ApJ*, 629, 915
 Belczynski K., Kalogera V., Bulik T., 2002, *ApJ*, 572, 407
 Belczynski K., Kalogera V., Rasio F. A., Taam R. E., Zezas A., Bulik T., Maccarone T. J., Ivanova N., 2005, *astro-ph/0511811*
 Benacquista M. J., Portegies Zwart S., Rasio F. A., 2001, *Classical and Quantum Gravity*, 18, 4025
 Chen K., Leonard P. J. T., 1993, *ApJL*, 411, L75
 Clark G. W., 1975, *ApJL*, 199, L143
 Cool A. M., Grindlay J. E., Cohn H. N., Lugger P. M., Bailyn C. D., 1998, *ApJL*, 508, L75
 Cool A. M., Grindlay J. E., Cohn H. N., Lugger P. M., Slavin S. D., 1995, *ApJ*, 439, 695
 Di Stefano R., Rappaport S., 1994, *ApJ*, 423, 274
 Dobrotka A., Lasota J.-P., Menou K., 2005, *ApJ* in press, *astro-ph/0509359*
 Edmonds P. D., Gilliland R. L., Heinke C. O., Grindlay J. E., 2003a, *ApJ*, 596, 1177
 Edmonds P. D., Gilliland R. L., Heinke C. O., Grindlay J. E., 2003b, *ApJ*, 596, 1197
 Edmonds P. D., Grindlay J. E., Cool A., Cohn H., Lugger P., Bailyn C., 1999, *ApJ*, 516, 250
 Fregeau J. M., Cheung P., Portegies Zwart S. F., Rasio F. A., 2004, *MNRAS*, 352, 1
 García-Senz D., Bravo E., Woosley S. E., 1999, *A&A*, 349, 177
 Grindlay J. E., Cool A. M., Callanan P. J., Bailyn C. D., Cohn H. N., Lugger P. M., 1995, *ApJL*, 455, L47
 Grindlay J. E., Heinke C., Edmonds P. D., Murray S. S., 2001, *Science*, 292, 2290
 Grindlay J. E., Heinke C. O., Edmonds P. D., Murray S. S., Cool A. M., 2001, *ApJL*, 563, L53
 Hakala P. J., Charles P. A., Johnston H. M., Verbunt F., 1997, *MNRAS*, 285, 693
 Hameury J.-M., Lasota J.-P., 2002, *A&A*, 394, 231
 Hannikainen D. C., Charles P. A., van Zyl L., Kong A. K. H., Homer L., Hakala P., Naylor T., Davies M. B., 2005, *MNRAS*, 357, 325
 Hansen B. M. S., Kalogera V., Rasio F. A., 2003, *ApJ*, 586, 1364
 Heggie D. C., Hut P., McMillan S. L. W., 1996, *ApJ*, 467, 359
 Heinke C. O., Grindlay J. E., Edmonds P. D., Cohn H. N., Lugger P. M., Camilo F., Bogdanov S., Freire P. C., 2005, *ApJ*, 625, 796
 Heinke C. O., Grindlay J. E., Lugger P. M., Cohn H. N., Edmonds P. D., Lloyd D. A., Cool A. M., 2003, *ApJ*, 598, 501
 Hurley J. R., Tout C. A., Pols O. R., 2002, *MNRAS*, 329, 897
 Ivanova N., 2006, *ApJ*, 636, 979
 Ivanova N., Belczynski K., Fregeau J. M., Rasio F. A., 2005, *MNRAS*, 358, 572
 Ivanova N., Fregeau J. M., Rasio F. A., 2005, in Rasio F. A., Stairs I. H., eds, *ASP Conf. Ser. 328: Binary Radio Pulsars Binary Evolution and Neutron Stars in Globular Clusters*. pp 231+
 Ivanova N., Rasio F., 2004, in *Revista Mexicana de Astronomia y Astrofisica Conference Series Compact Binaries in Globular Clusters*. pp 67–70
 Ivanova N., Rasio F. A., 2005, in Burderi L., Antonelli L. A., D'Antona F., di Salvo T., Israel G. L., Piersanti L., Tornambè A., Straniero O., eds, *AIP Conf. Proc. 797: Interacting Binaries: Accretion, Evolution, and Outcomes Formation and evolution of compact binaries with an accreting white dwarf in globular clusters*. pp 53–60
 Ivanova N., Rasio F. A., Lombardi J. C., Dooley K. L., Proulx Z. F., 2005, *ApJL*, 621, L109
 Ivanova N., Taam R. E., 2003, *ApJ*, 599, 516
 Ivanova N., Taam R. E., 2004, *ApJ*, 601, 1058
 Kaluzny J., Pietrukowicz P., Thompson I. B., Krzeminski W., Schwarzenberg-Czerny A., Pych W., Stachowski G., 2005, *MNRAS*, 359, 677
 Kaluzny J., Thompson I. B., 2003, *AJ*, 125, 2534
 Kato M., Hachisu I., 1999, *ApJL*, 513, L41
 Kim D.-W., Fabbiano G., 2004, *ApJ*, 611, 846
 Knigge C., Zurek D. R., Shara M. M., Long K. S., Gilliland R. L., 2003, *ApJ*, 599, 1320
 Kroupa P., 2002, *Science*, 295, 82
 Leibundgut B., 2001, *ARAA*, 39, 67

- Levan A. J., Wynn G. A., Chapman R., Davies M. B., King A. R., Priddey R. S., Tanvir N. R., 2006, *MNRAS*, pp L15+
- Liebert J., Bergeron P., Holberg J. B., 2003, *AJ*, 125, 348
- Livne E., Glasner A. S., 1991, *ApJ*, 370, 272
- Lombardi J. C., Proulx Z. F., Dooley K. L., Theriault E. M., Ivanova N., Rasio F. A., 2006, *ApJ* accepted
- Mannucci F., Della Valle M., Panagia N., Cappellaro E., Cresci G., Maiolino R., Petrosian A., Turatto M., 2005, *A&A*, 433, 807
- Mardling R. A., 1995, *ApJ*, 450, 732
- Neill J. D., Shara M. M., Caulet A., Buckley D. A. H., 2002, *AJ*, 123, 3298
- Nelemans G., Portegies Zwart S. F., Verbunt F., Yungelson L. R., 2001, *A&A*, 368, 939
- Patterson J., Raymond J. C., 1985, *ApJ*, 292, 535
- Pfahl E., Rappaport S., Podsiadlowski P., 2002, *ApJ*, 573, 283
- Pietrukowicz P., Kaluzny J., Thompson I. B., Jaroszynski M., Schwarzenberg-Czerny A., Krzeminski W., Pych W., 2005, *Acta Astronomica*, 55, 261
- Podsiadlowski P., Langer N., Poelarends A. J. T., Rappaport S., Heger A., Pfahl E., 2004, *ApJ*, 612, 1044
- Pooley D., Lewin W. H. G., Anderson S. F., et al. 2003, *ApJL*, 591, L131
- Pooley D., Lewin W. H. G., Homer L., et al. 2002, *ApJ*, 569, 405
- Portegies Zwart S. F., Meinen A. T., 1993, *A&A*, 280, 174
- Rappaport S., Verbunt F., Joss P. C., 1983, *ApJ*, 275, 713
- Rodríguez-Gil P., Casares J., Martínez-Pais I. G., Hakala P., Steeghs D., 2001, *ApJL*, 548, L49
- Scannapieco E., Bildsten L., 2005, *ApJL*, 629, L85
- Shara M. M., Bergeron L. E., Gilliland R. L., Saha A., Petro L., 1996, *ApJ*, 471, 804
- Shara M. M., Drissen L., 1995, *ApJ*, 448, 203
- Shara M. M., Hinkley S., Zurek D. R., Knigge C., Dieball A., 2005, *AJ*, 130, 1829
- Shara M. M., Hurley J. R., 2002, *ApJ*, 571, 830
- Stroeer A., Vecchio A., Nelemans G., 2005, *ApJL*, 633, L33
- Taam R. E., 1980, *ApJ*, 242, 749
- Vennes S., 1999, *ApJ*, 525, 995
- Verbunt F., Bunk W. H., Ritter H., Pfeffermann E., 1997, *A&A*, 327, 602
- Whitehurst R., King A., 1991, *MNRAS*, 249, 25
- Wickramasinghe D. T., Ferrario L., 2005, *MNRAS*, 356, 1576
- Woosley S. E., Weaver T. A., 1994, *ApJ*, 423, 371